

# Reaction-diffusion with stochastic decay rates

G. John Lapeyre Jr.<sup>1,2</sup> and Marco Dentz<sup>1</sup>

<sup>1</sup>*Spanish National Research Council (IDAEA-CSIC), E-08034 Barcelona, Spain*

<sup>2</sup>*ICFO–Institut de Ciències Fotòniques, Mediterranean Technology Park, 08860 Castelldefels, Spain*

(Dated: March 11, 2018)

Understanding anomalous transport and reaction kinetics due to microscopic physical and chemical disorder is a long-standing goal in many fields including geophysics, biology, and engineering. We consider reaction-diffusion characterized by fluctuations in both transport times and decay rates. We introduce and analyze a model framework that explicitly connects microscopic fluctuations with the mesoscopic description. For broad distributions of transport and reaction time scales we compute the particle density and derive the equations governing its evolution, finding power-law decay of the survival probability, and spatially varying decay that leads to subdiffusion and an asymptotically stationary surviving-particle density. These anomalies are clearly attributable to non-Markovian effects that couple transport and chemical properties in both reaction and diffusion terms.

## I. INTRODUCTION

Due to the interaction of diffusion and reaction mechanisms, reaction-diffusion systems in fluctuating environments may develop collective behaviors that are very different from those occurring under well mixed conditions. Smoluchowski’s theory [1] quantifies the interaction of diffusion and reaction for fast bimolecular reactions through an effective rate that is proportional to the molecular diffusion coefficient. This approach is valid under well-mixed conditions. Spatial and temporal fluctuations may lead to the segregation of the reactants [2] characterized by non-Poissonian encounter processes and broad first-passage time distributions [3–5], such that reaction kinetics on small and large scales may be very different [6]. The sound understanding and quantification of the mechanisms by which heterogeneity on small scales leads to “non-classical” or “anomalous” kinetics on large scales plays a central role in applications as diverse as contaminant degradation and chemical transformations in geological media [7, 8] and chemical kinetics in crowded intracellular environments [9]. A number of approaches have been proposed to model reaction behaviors in heterogeneous environments, including fractional kinetic orders and time-dependent rate coefficients [10, 11] as well as delayed-reaction equations [9, 12–14]. Oftentimes, such effective approaches to explain non-exponential survival probabilities are phenomenology-based lumped parameter models [15]. Indeed, the variety of mechanisms leading to anomalous diffusion and kinetics precludes general answers to fundamental questions. For instance, are emergent anomalous kinetics better described by non-linear, or by non-Markovian evolution equations? We address this question by solving the random decay model for fluctuations characterized by broad distributions of transport and reaction time scales, obtaining reaction-subdiffusion equations. Insisting on an exact derivation is especially important in this case, since the *prima facie* reasonable approach of adding reaction terms to known subdiffusion equations [16–21] has been shown to be inconsistent with microscopic dynamics and kinetics [22].

We find anomalous kinetics associated with population splitting and identify the cause in non-Markovian, rather than non-linear effects. Furthermore, the transport is highly anomalous, with the particle density approaching a stationary state.

We do not make assumptions regarding the origin of the distribution of transport times, but rather take these properties as given. However, it is important to note there do exist derivations in the literature of transport properties, such as first-passage times, from characteristics of complex media. For instance, first-passage observables have been computed for diffusion on fractals or media with heavy-tailed trap distributions [3], and by applying the mapping between random walks and vibrations to complex elastic networks [4, 5].

The paper is organized as follows. In Sec. II we introduce the random decay model as the continuous time random walk (CTRW) in which the walker is subject to a random decay process during each waiting period. In Sec. III, we derive the generalized master equation for the particle density and derive the solution in Fourier-Laplace space. In Sec. IV, we connect the random rate model to a general stochastic process. We preview the main results in this connection: the mean square displacement approaches a constant. The reaction kinetics follow a power law governed by an evolution equation with a heavy-tailed memory kernel that couples microscopic transport and reaction parameters. In Sec. VA, we show that ordinary diffusion subject to random decay leads to perfect mixing in the scaling limit, and is equivalent to decay at a single, average rate. In Sec. VB, we consider random rates combined with heavy-tailed waiting times and derive a generalized fractional Fokker-Planck reaction-diffusion equation with reaction and diffusion kernels that couple reaction and transport. In Sec. VC, we assume a power-law rate PDF and derive exact asymptotic expressions for the reaction-diffusion equations and solutions. In Sec. VI, we demonstrate localization by deriving the exact expression for the asymptotic, steady-state particle density as a two-sided exponential distribution.

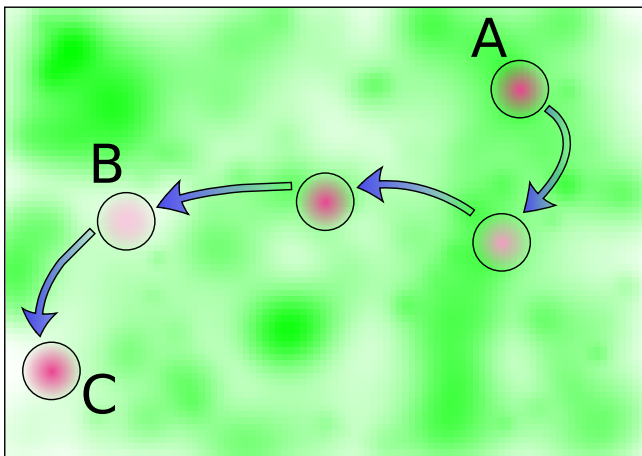


FIG. 1. Overview of the model. The particle makes random jumps until it decays. Darker green corresponds to faster jumping. Darker red corresponds to faster decay. For clarity, the decay rate (red) is shown only at sites that the walker occupies. (A) Dark green and dark red: the particle experiences a high decay rate for a short time. (B) Light green and light red: The particle is immobile for a long time with a small decay rate, and so may survive for a long time. Events like (B) cause anomalous kinetics. (C) Light green and dark red: Particle is immobile for a long time with high decay rate, and so has a high probability of decaying in this step.

## II. THE RANDOM DECAY MODEL

### A. Stochastic decay rates

In this section, we formulate our model of diffusion in a fluctuating physical and chemical environment as a continuous time random walk (CTRW) subject to random decay. That is, a particle of species  $A$  performs a random walk and at the same time, undergoes an irreversible reaction  $A \rightarrow B$ . The particle waits a random time  $\tau$  before making each step, and undergoes decay at a rate  $\rho$  during this waiting period, where  $\tau$  and  $\rho$  vary randomly. Regions where long waiting times and slow decay coincide are responsible for subdiffusion and anomalous kinetics, as illustrated in Fig. 1. This type of quenched disorder in the reaction and diffusion properties may occur in heterogeneous geological media characterized by a spatial distribution of minerals and thus specific reactive surface, and porosity [7], which leads to scale effects in the reaction properties [23, 24].

In this paper, we aim at quantifying the impact of variability in the physical and chemical system properties on the reaction behavior. To this end, we make the simplifying assumption that each random waiting time is independent of all past waiting times, and each decay rate is independent of all past decay rates. In other words, we assume fully annealed disorder, ignoring possible effects of correlations between steps. Models of quenched disorder assume that the medium fluctuates slowly enough that the walker samples a static configuration. However,

annealed disorder is inherent in many systems in which the timescales of thermal fluctuations and stochastically varying transport and kinetic parameters are not well separated. For example, the waiting times may arise from long excursions into cul-de-sacs where the duration of the excursion is due to the motion of the particle itself, and so is memoryless. This feature has been exploited in studying reaction-subdiffusion front propagation in spiny dendrites [25]. Furthermore, the stochasticity may stem from a fluctuating internal state of a particle that interacts with the medium. Examples of the latter are conformational fluctuations of proteins [26] and enzymes [27]. It is worth noting that, in distinction from quenched models, annealed models are often solvable. In some cases, these solutions provide insight into features of the corresponding quenched model that do not depend strongly on correlations. This is the case for the model considered here. We derive exact results showing anomalous kinetics due to memory effects. Preliminary numerical results show that exponents characterizing power-law behavior of the mean square displacement (MSD) and survival probability are the same in annealed and quenched versions of the model [28], which suggests that the same memory effects are at play in the quenched setting.

The structure of the annealed model allows the following practical simplification, and at the same time, generalization. During the  $n$ th step, the particle is subject to two random processes, one triggering spatial translation and the other the conversion from species  $A$  to species  $B$ . For example, the waiting time before translation may be due to thermally driven escape from a trap with random energy. And the reaction rate may depend on the random local concentration of a catalyst. Escape from the trap will interrupt the reaction. And reaction will effectively interrupt escape by removing the particle from the population whose concentration we are measuring. Since one can view the jumping as interrupting an ongoing reaction and starting a new one, the  $n$ th step may be simulated as follows. Sample a waiting time  $\tau^*$  from the PDF of  $\tau$  and a rate  $r$  from the PDF of  $\rho$ . Then, sample a random decay time  $t$  from the PDF

$$\psi_r(t|r) = r \exp(-tr). \quad (1)$$

If  $\tau^* < t$ , the reaction is interrupted and the particle jumps. On the other hand, if  $t \leq \tau^*$ , the particle indeed decays. But, sampling first a decay rate, and then a decay time is mathematically equivalent to sampling the decay time directly from the PDF of a single-step decay time  $\Delta$  given by

$$\psi_\Delta(t) = \int_0^\infty dr \psi_r(t|r) \psi_\rho(r), \quad (2)$$

where  $\psi_\rho(r)$  is the PDF of  $\rho$ . It is worth noting that this procedure is equivalent to sampling a decay time from a PDF  $\psi_\Delta(t)$  that is *independent* of the step number  $n$ . In other words, Poissonian decay with a random parameter (the rate) is equivalent to non-Poissonian decay described

a single PDF. In fact the argument above also works if 1)  $\Delta$  is due to averaging an arbitrary PDF over a random parameter, and 2)  $\tau$  and  $\Delta$  are not independent. In the following, we derive the basic results in this generality for two reasons. Firstly, the results may be applied directly to more complicated situations. For example, we will suggest below a stochastic Michaelis-Menten scheme defined by coupling  $\Delta$  and  $\tau$ . Secondly, as we discuss below, results from the study of a broad class of stochastic processes can be applied directly to the general formulation of our model [29].

## B. General formulation

We consider a molecular entity of type  $A$  (the ‘‘particle’’) performing a continuous-time random walk while undergoing random conversion to an entity of type  $B$ . The particle’s position  $x_n$  and time  $t_n$  are given by

$$x_{n+1} = x_n + \xi_{n+1}, \quad t_{n+1} = t_n + \tau_{n+1}, \quad (3)$$

where  $n \geq 0$ ,  $t_0 = 0$ , and the initial density, that is the density of  $x_0$  is denoted  $p_0(x)$ . Here,  $\tau_n$  is the random waiting time before the  $n$ th step, and  $\xi_n$  is the step displacement. We call the time interval  $[t_n, t_n + \tau_{n+1}]$  the  $n$ th *renewal period*. The particle position at time  $t$  is then given by

$$x(t) = x_{n_t}, \quad (4)$$

where the renewal process  $n_t = \max(n | t_n \leq t)$  is the number of steps (renewal periods) taken by time  $t$ . With each renewal period, we associate a single-step random decay time  $\Delta_n$ . The decay time  $\Delta_n$  may be due to a disordered Poissonian process as in (2) or some more complicated chemical or biological process. It represents the time it would take the particle to decay if it were not subject to transport. Thus, if the particle is still alive at time  $t_n$  and  $\tau_n < \Delta_n$ , then the particle takes the  $n$ th step before it decays, and thus survives decay. On the other hand, if  $\Delta_n \leq \tau_n$ , then the particle decays before it has a chance to take a step. The random renewal period  $m$  during which the particle decays is given by  $m = \min(n | \Delta_n < \tau_n)$ . Thus, the random time  $S$  at which the particle finally decays after zero or more periods is given by

$$S = \sum_{n=1}^{m-1} \tau_n + \Delta_m. \quad (5)$$

Note that the clock  $t_n$  tracks only the step waiting times, but not the decay time. The analysis is facilitated by this choice, that is, considering an ordinary CTRW for which we mark the special time  $S$ . Note also, that this framework is different from kinetic Monte-Carlo approaches such as the (spatial) Gillespie method [30, 31], which treats both diffusive and reactive particle events on the same ground. In the present work, particles perform a

spatial random walk according to (3), and they may react during the (physical) waiting time with a certain probability as detailed above. This approach is equivalent to the reaction-diffusion equation for the species concentration [22] and to more general non-local reaction and reaction-diffusion equations as developed in the remainder of the paper.

We assume annealed disorder, so that each renewal period is independent. That is,  $(\xi_n, \tau_n, \Delta_n)$ ,  $n = 1, 2, \dots$  are independent and identically distributed (iid) copies of  $(\xi, \tau, \Delta)$ . For the moment, we allow that  $\tau$  and  $\Delta$  may be dependent as they may be coupled by chemical and physical properties of the medium. Although we mention such situations in Sec. IX, for the bulk of the paper, we will assume that they are uncoupled. For simplicity we assume that the step displacement  $\xi$  is independent of both  $\Delta$  and  $\tau$  and is distributed according to the probability density function (PDF)  $\psi_\xi(x)$  satisfying

$$\langle \xi \rangle = 0, \quad \langle \xi^2 \rangle = \delta^2 < \infty, \quad (6)$$

where angle brackets denote averages and  $\delta$  is a microscopic length scale characterizing the typical jump length. In this paper we distinguish Laplace transformed quantities by a hat, and Fourier transformed quantities by a tilde. The Laplace-conjugate of  $t$  is  $s$  and the Fourier-conjugate of  $x$  is  $k$ .

The use of the word *coupled* above refers only to whether random variables representing microscopic quantities are independent. Below, we shall be concerned with whether the mesoscopic transport and reaction are coupled. There is no direct relation between these two concepts. In fact, we find mesoscopic coupling in the case that all microscopic random variables are independent.

It is worth noting that the random decay time  $S$  takes the form of the generic first passage time (FPT) under reset [29, 32]. Here the ‘‘passage’’ is completion of a reaction (decay) at time  $\Delta$ , and the reset time  $\tau$  begins the reaction anew. Thus, the random decay model may be viewed as FPT under reset coupled with CTRW by identifying the reset time of the FPT with the waiting time of the CTRW. The identification of the survival time  $S$  with FPT under reset allows one to immediately apply general results for FPT under reset [29], including expressions for the mean FPT and fluctuations.

The main quantities of interest are the following. We refer to the probability that the particle has not decayed up to time  $t$  as the *survival* probability, denoted by

$$p(t) = \Pr(t < S). \quad (7)$$

The evolution of  $p(t)$  gives information on the chemical kinetics and reaction dynamics averaged over the entire system. For example, under a constant decay rate  $\rho_0$ , it decays exponentially as  $p(t) = \exp(-\rho_0 t)$ . The density of surviving particles is given by the particle density of the CTRW conditioned on survival, that is, on  $t < S$ . We denote the density of surviving particles by

$$p(x, t | t < S). \quad (8)$$

Recall that we use the word “decay” as a shorthand for any irreversible reaction  $A \rightarrow B$ . Since we assume that the entities are non-interacting, one may interpret  $p(x, t|t < S)$  as either the probability density for a single  $A$  entity, or as the local concentration or number density of  $A$  normalized to one. In the latter case,  $p(x, t|t < S)$  is the profile observed at time  $t$  by an imaging technique that detects species  $A$ , but not species  $B$ . According to Bayes’ rule and (7), the joint particle density and probability of survival is then given by

$$p(x, t) = p(x, t|t < S)p(t). \quad (9)$$

For simplicity, we shall refer to  $p(x, t)$  as a “density”. Because  $p(x, t|t < S)$  is normalized to one, we have the marginal

$$\int_{-\infty}^{\infty} p(x, t) dx = p(t). \quad (10)$$

Although  $p(t)$  and  $p(x, t|t < S)$  are the physically relevant quantities,  $p(x, t)$  is more accessible mathematically. Thus, we will calculate  $p(x, t)$  and obtain  $p(x, t|t < S)$  via (9) by dividing by  $p(t)$ . The mean square displacement  $m(t)$ , given by

$$m(t) = \int_{-\infty}^{\infty} x^2 p(x, t|t < S) dx, \quad (11)$$

measures the spatial extent of the surviving particles.

Finally, it is important to note that we focus on rate PDFs with a finite probability that the rate is either zero, or arbitrarily close to zero. This is because the anomalous behaviour is driven by the coincidence of very long waiting times with very long decay times. In Sec. VIII, we discuss how the anomalies are modified in the case that the minimum possible rate is greater than zero.

### III. GENERALIZED MASTER EQUATION AND SOLUTION

We derive the generalized master equation [33] and solution for the random decay model. The particle density  $p(x, t)$  defined in (9) satisfies (See Sec. X A.)

$$p(x, t) = \int_0^t dt' \eta(x, t') \Phi_{\tau\Delta}(t - t'). \quad (12a)$$

Here  $\eta(x, t)$  is the incoming live-particle flux at position  $x$  at time  $t$ . That is,  $\eta(x, t) dx dt$  is the probability that the particle is alive and makes a step between times  $t$  and  $t + dt$  into the region between  $x$  and  $x + dx$  And the factor

$$\Phi_{\tau\Delta}(t - t') \equiv \Pr(t - t' < \min[\tau, \Delta]), \quad (12b)$$

is the probability that the particle has survived both translation (i.e. has not escaped from a trap) and decay

up to time  $t$  during a renewal period beginning at time  $t'$ . Thus, the integral counts all particles that arrived at  $x$  at some time  $t'$  in the past and that have neither jumped away, nor decayed in the time  $t - t'$  since arriving. The flux  $\eta(x, t)$  satisfies the Chapman-Kolmogorov type integral equation

$$\eta(x, t) = \int_{-\infty}^{\infty} dx' \int_0^{\infty} dt' \eta(x', t') \psi_{\xi}(x - x') \phi_{\tau\Delta}(t - t') + p_0(x) \delta(t), \quad (12c)$$

where

$$\phi_{\tau\Delta}(t) \equiv \psi_{\tau}(t|t < \Delta) \Pr(t < \Delta), \quad (13)$$

is the joint probability and probability density to survive both translation and single-step decay until time  $t$  and then to make a translation (jump) at time  $t$ . Here  $\psi_{\tau}(t|t < \Delta) = \langle \delta(t - \tau) | t < \Delta \rangle$  is the PDF of the waiting time  $\tau$  conditioned on waiting time smaller than decay time,  $t < \Delta$ . Eq. (13) expresses particle balance under reaction losses. Note that Eqs. (12a) and (12c) have the same structure as the governing equations of the classical CTRW. But in fact they do not describe a CTRW and the model cannot be cast as one. This is due to the presence of reactions, with the result that  $\phi_{\tau\Delta}(t)$  is not a waiting time PDF and  $\Phi_{\tau\Delta}(t)$  is not a translation survival probability. Instead the decay of the single-step survival probability  $\Phi_{\tau\Delta}(t)$  includes two loss terms representing translations and decay. Taking the derivative of (12b) we find

$$\partial_t \Phi_{\tau\Delta}(t) = -\phi_{\tau\Delta}(t) - \phi_{\Delta\tau}(t), \quad (14)$$

where

$$\phi_{\Delta\tau}(t) \equiv \psi_{\Delta}(t|t \leq \tau) \Pr(t \leq \tau), \quad (15)$$

is the joint probability to both survive single-step decay and not make a jump until time  $t$ , and then to decay at time  $t$ .

The system (12) can be combined into the generalized reaction-diffusion Master equation (GME) (See Sec. X B.)

$$\begin{aligned} \frac{\partial p(x, t)}{\partial t} = & - \int_0^t dt' \mathcal{K}_r(t - t') p(x, t') + \\ & \int_{-\infty}^{\infty} dx' \int_0^t dt' \mathcal{K}_d(t - t') \psi_{\xi}(x - x') [p(x', t') - p(x, t')], \end{aligned} \quad (16)$$

where we define the reaction kernel  $\mathcal{K}_r(t)$  and the diffusion kernel  $\mathcal{K}_d(x, t)$  through their Laplace transforms as

$$\hat{\mathcal{K}}_r(s) = \frac{\hat{\phi}_{\Delta\tau}(s)}{\hat{\Phi}_{\tau\Delta}(s)}, \quad \hat{\mathcal{K}}_d(s) = \frac{\hat{\phi}_{\tau\Delta}(s)}{\hat{\Phi}_{\tau\Delta}(s)}. \quad (17)$$



The diffusion kernel quantifies the impact of random decay and waiting times on the spatial motion, the reaction kernel on the particle survival. As is evident in the kernels, the reaction and transport processes are intimately coupled.

Integration of (16) over space reveals the dynamics that govern the reaction kinetics,

$$\frac{dp(t)}{dt} = - \int_0^t dt' \mathcal{K}_r(t-t')p(t'). \quad (18)$$

Eq. (18) is of central importance. It expresses the impact of segregation of the reactants and the different reaction and transport histories on the overall reaction behavior. The Markov property of the reaction process that underlies the exponential model breaks down in the presence of distributed reaction and diffusion rates. It is interesting to note that the Gillespie method [30] is a fully Markovian method, in which interreaction waiting times are exponentially distributed. The non-local nature of 18 indicates that this is no longer valid in spatially heterogeneous systems. This is the subject of ongoing work.

The solution to the GME in Fourier-Laplace space is the generalized Montroll-Weiss equation for the particle density (See Sec. XC 1.)

$$\hat{p}(k, s) = \frac{\hat{\Phi}_{\tau\Delta}(s)\tilde{p}_0(k)}{1 - \tilde{\psi}_\xi(k)\hat{\phi}_{\tau\Delta}(s)}. \quad (19)$$

Note that (19) involves  $\phi_{\tau\Delta}(t)$  defined in (13) and  $\Phi_{\tau\Delta}(t)$  defined in (12b), but not  $\phi_{\Delta\tau}(t)$  defined in (15). This is because both  $\phi_{\tau\Delta}(t)$  and  $\Phi_{\tau\Delta}(t)$  characterize the event that decay does not occur, while  $\phi_{\Delta\tau}(t)$  characterizes the event that decay *does* occur. This is to be expected, since  $p(x, t)$  is the density of particles that have not decayed.

Setting  $k = 0$  in Fourier space is equivalent to integrating over  $x$  in real space. Thus, putting  $k = 0$  in (19) and referring to (10), we obtain the expression for the survival probability

$$\hat{p}(s) = \frac{\hat{\Phi}_{\tau\Delta}(s)}{1 - \hat{\phi}_{\tau\Delta}(s)}.$$

The mean survival time  $\langle S \rangle$  is given by  $\langle S \rangle = \hat{p}(0)$ , from which we obtain the simple form

$$\langle S \rangle = \frac{\langle \min(\tau, \Delta) \rangle}{\text{Pr}(\Delta < \tau)}. \quad (20)$$

As mentioned above, the survival time  $S$  is formally a FPT under reset. A simple, alternative derivation of (20) from this viewpoint is found in Ref. [29]. From (20) we see that  $\langle S \rangle$  increases with 1) increasing probability of large values of both  $\Delta$  and  $\tau$ , and 2) increasing probability of  $\Delta > \tau$ .

#### IV. STOCHASTIC RATES AND ANOMALOUS KINETICS

We now assume that the single-step decay time and the translation waiting time are uncoupled, that is,  $\tau$  and  $\Delta$

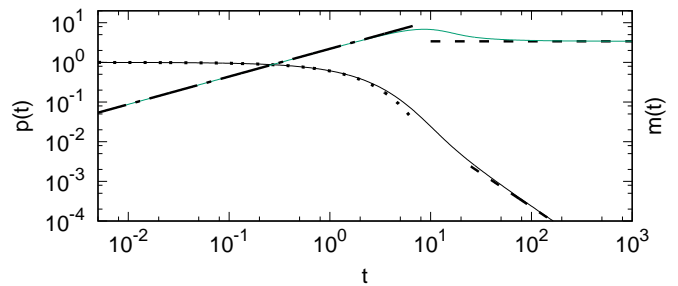


FIG. 2. (Black solid) Survival probability  $p(t)$  and (green solid) mean square displacement  $m(t)$  defined in (11) for heavy-tailed waiting time PDF, and power-law reaction rate PDF with  $\alpha = 0.7$ ,  $\nu = 1$ , and  $\tau_r = 1$ . Left and right ordinate axes differ in physical dimensions, but are numerically equal. (Dotted) Exponential short time behavior of the survival probability, which is characterized by the average rate  $\langle \rho \rangle$ . (Lower dashed) Asymptotic power-law decay  $p(t) \propto t^{-\gamma}$ . (Dash-dotted) Short-time power-law behavior  $m(t) \propto t^\alpha$ . (Upper dashed) Asymptotically constant  $m(t)$  occurring on the localization time scale  $\langle \rho^\alpha \rangle^{-1/\alpha}$ .

are independent. We denote the PDF of waiting times  $\tau$  by

$$\psi_\tau(t) \equiv \tau_m^{-1} \bar{\psi}_\tau(t/\tau_m), \quad (21)$$

where  $\bar{\psi}_\tau(z)$  is dimensionless and  $\tau_m$  is the waiting time scale. Furthermore, we adopt the viewpoint of Sec. II A that the randomness in decay is due to first-order decay with rates that vary stochastically, but are constant during each renewal period. The variability in rates is characterized by the PDF

$$\psi_\rho(r) \equiv \tau_r \bar{\psi}_\rho(r/\tau_r), \quad (22)$$

where  $\tau_r$  is the time scale of single-step decay, and  $\bar{\psi}_\rho(z)$  is a dimensionless PDF.

A main result and key message of this paper is that strong physical disorder expressed via (21) combined with disordered rates expressed via (22) leads to anomalous kinetics as well as anomalies in transport beyond standard subdiffusion. We quantify these anomalies and identify their source in long reaction memory rather than nonlinearity. The anomalous kinetics and transport are clearly evident in Fig. 2, which shows the survival probability  $p(t)$  and the mean square displacement  $m(t)$  for a heavy-tailed waiting time PDF that behaves as  $\psi_\tau(t) \propto t^{-1-\alpha}$  with  $0 < \alpha < 1$ , for  $t$  larger than the characteristic time  $\tau_m$  in (21), and a rate PDF that behaves as  $\psi_\rho(r) \propto r^{\nu-1}$  with  $\nu > 0$  for  $r$  smaller than the characteristic rate  $1/\tau_r$ . We observe two remarkable behaviors. Firstly, the survival probability decays as a power-law  $p(t) \propto t^{-\gamma}$ , where

$$\gamma = \alpha + \nu, \quad (23)$$

and secondly,  $m(t)$  increases proportionally to  $t^\alpha$ , as for non-reacting particles, until a characteristic reaction time

scale after which it decays towards a constant. These two behaviors indicate a localization of the density of surviving particles.

The power-law decay of the survival probability observed in Fig. 2 can be modeled by a non-linear kinetic rate law as [10]

$$\frac{dp(t)}{dt} = -k_e p(t)^{\frac{1+\gamma}{\gamma}} \quad (24)$$

with  $k_e$  as an effective reaction rate. While this equation gives the power-law decay  $p(t) \propto t^{-\gamma}$ , it implies a conceptual framework that is clearly inconsistent with the correct evolution equation (18). Indeed (18) is linear but non-Markovian, implying history-dependent evolution. This is an important point as the conceptual framework influences the approach taken to more complicated scenarios. A discussion of its importance in interpreting experiments is found in Ref. [34].

## V. REACTION-DIFFUSION DYNAMICS

Spatial fluctuations in biological and physical systems provide our main motivation for assuming that the random decay has its origin in disordered rates. Thus, in the following analysis we assume that the single-step decay time  $\Delta$  arises from averaging decay over random rates. However, it may be useful to go in the opposite direction. Given a distribution for  $\Delta$ , compute the corresponding distribution rates. In this way our results, although explicitly written in terms of random rates, may be applied to random decay times  $\Delta$  of varying physical origin. The PDF  $\psi_\rho(r)$  is obtained from that of  $\Delta$  as follows. Referring to (1), it is easy to see that the single-step decay-survival probability is given by

$$\Pr(t < \Delta) = \langle e^{-\rho t} \rangle. \quad (25)$$

Since (25) is the Laplace transform of  $\rho$ , it may be inverted for any density of  $\Delta$  for which the inverse Laplace transform exists.<sup>1</sup>

We begin by writing the GME in terms of random rates. Using the independence of  $\tau$  and  $\Delta$  and referring to (25), we find  $\hat{\phi}_{\tau\Delta}(s) = \langle \hat{\psi}_\tau(s + \rho) \rangle$ ,  $\hat{\phi}_{\Delta\tau}(s) = \langle \rho \hat{\Psi}_\tau(s + \rho) \rangle$ , and  $\hat{\Phi}_{\tau\Delta}(s) = \langle \hat{\Psi}_\tau(s + \rho) \rangle$ , where the translation survival probability  $\Psi_\tau(t) = \Pr(t < \tau)$  is given by

$$\Psi_\tau(t) = \int_t^\infty \psi_\tau(t') dt'. \quad (26)$$

$\Psi_\tau(t)$  is the probability, in the absence of decay, that the particle has not taken a step during a renewal period

before time  $t$ . Thus, the solution (19) to the GME (16) may be written as

$$\hat{p}(k, s) = \frac{\tilde{p}_0(k) \langle \hat{\Psi}_\tau(s + \rho) \rangle}{1 - \tilde{\psi}_\xi(k) \langle \hat{\psi}_\tau(s + \rho) \rangle}. \quad (27)$$

Eq. (27) is the basis of the following analysis. We will describe the conditions under which on the one hand, the system becomes well-mixed and exhibits homogeneous kinetics at long times, and on the other hand the system remains poorly-mixed and exhibits persistent physical and chemical anomalies. In the following, we assume that the rate density (22) has weight at, or in the neighborhood of,  $r = 0$ , leaving the more general case to Sec. VIII.

The main factors determining the evolution of  $p(t)$  and  $p(x, t)$ , and the degree of mixing in particular are 1) whether the mean waiting time between jumps exists, ie  $\langle \tau \rangle < \infty$ . 2) The relative magnitude of the three time scales: the time scale of microscopic transport  $\tau_m$  defined in (21), the time scale of reactions  $\tau_r$  from (22), and the physical time  $t$ . If  $\langle \tau \rangle < \infty$ , and

$$\tau_m < \tau_r < t, \quad (28)$$

then the system tends to a well-mixed state with homogeneous kinetics as the time scales separate. This is because at long times surviving particles have typically made many steps and will sample many rates before dying. On the other hand, if  $\langle \tau \rangle$  diverges, then the system never becomes well mixed, no matter how large the scale separation in (28). Instead, we find anomalous kinetics and dynamics due to memory effects. This corresponds to particles that are trapped for long times in regions of low reactivity.

### A. Well-mixed scenario.

We first treat the case  $\langle \tau \rangle < \infty$ . We consider the scaling limit in order obtain a mesoscopic picture in which observational length and time scales are much larger than the microscopic scales. In the scaling limit  $\delta \rightarrow 0$  and  $\tau_m \rightarrow 0$  such that

$$\mathcal{D} = \delta^2 / (2\tau_m) \quad (29)$$

converges to a positive constant, the GME (16) reduces to

$$\frac{\partial p(x, t)}{\partial t} = -\langle \rho \rangle p(x, t) + \mathcal{D} \frac{\partial^2 p(x, t)}{\partial x^2}, \quad (30)$$

provided  $\langle \rho \rangle < \infty$ . (See Sec. XD.) Eq. (30) gives a mesoscopic description of evolution of the system. The local density changes little over a short time, but this time represents an infinite number of steps. Of course, physically, displacements and waiting times may be very small, but must be finite. Thus, eq. (30) is an accurate description insofar as the microscopic and observational physical scales are well separated. For a colloidal system,

<sup>1</sup> An example of a single-step decay-survival probability that does not have a Laplace inverse, and thus cannot be expressed via random rates, is a deterministic decay time  $\psi_\Delta(t) = \delta(t - \Delta_0)$ .

the waiting time is the time between collisions of solvent molecules with a relatively massive particle, so that the ratio of the time required for the particle to move a distance equal to its own radius and the time between collisions may be 6 orders of magnitude or more. On the other hand, if the waiting times are dominated by trapping, then the timescale of the trapping  $\tau_r$  plays the role of the microscopic time scale and the separation between  $\tau_r$  and the mesoscopic scale may not be as large. We present an example of the latter case for  $\langle\tau\rangle = \infty$  in Sec. XF.

In the present case, (30) describes ordinary diffusion with a constant, homogeneous decay rate. The survival probability  $p(t)$  satisfies the first-order rate equation

$$\frac{dp(t)}{dt} = -\langle\rho\rangle p(t). \quad (31)$$

The effective reaction kinetics are determined solely by the characteristic reaction rate. Eq. (30) makes evident that on the mesoscopic level the kinetics are effectively homogeneous in space. Note that this behavior is also observed in general at times shorter than both the reaction and translation time scales  $\tau_r$  and  $\tau_m$ . In this case, the reaction kernel also reduces to  $\hat{\mathcal{K}}_r(s) = \langle\rho\rangle$ . This is obtained from (17) by considering the limit  $s \gg 1/\tau_r$  and  $s \gg 1/\tau_m$ .

The scaling limit leading to (29) and (30) involves letting  $\tau_m$  approach zero. Since we do not rescale the reactions, this implies  $\tau_m \ll \tau_r$ , which corresponds to a small Damköhler number. Eq. (31) immediately gives us the mean survival time  $\langle S \rangle = \langle\rho\rangle^{-1}$ . The extreme opposite to the scaling limit is  $\tau_r \ll \tau_m$  and corresponds to large Damköhler number. In this case, the mean survival time is just the mean single-step decay time  $\langle\Delta\rangle$ . This can be seen by noting that for  $\tau_r \ll \tau_m$  it is highly probable that  $\Delta < \tau$ . Thus, the numerator in (20) is approximately  $\langle\Delta\rangle$  and the denominator approximately 1. Furthermore, we note that  $\langle\Delta\rangle = \int_0^\infty dt \Pr(t < \Delta)$ , and use (25) to arrive at

$$\langle S \rangle \approx \langle\Delta\rangle = \langle\rho^{-1}\rangle, \quad \tau_r \ll \tau_m, \quad (32)$$

provided the moment exists. There is no mixing at all, and  $\langle S \rangle$  is dominated by particles that never jump, but instead decay in their initial environments. The intermediate behavior between these extremes depends strongly on details of the distributions of both the rate and of the waiting-times, rather than just their asymptotics. We defer a discussion of these more complicated and varied results to Sec. XE.

## B. Fractional reaction-diffusion.

As discussed in the Introduction and indicated in Figs. 1 and 2, broad waiting time distributions lead to anomalously long particle survivals if they coincide with small or vanishing reaction rates. This inhibits mixing

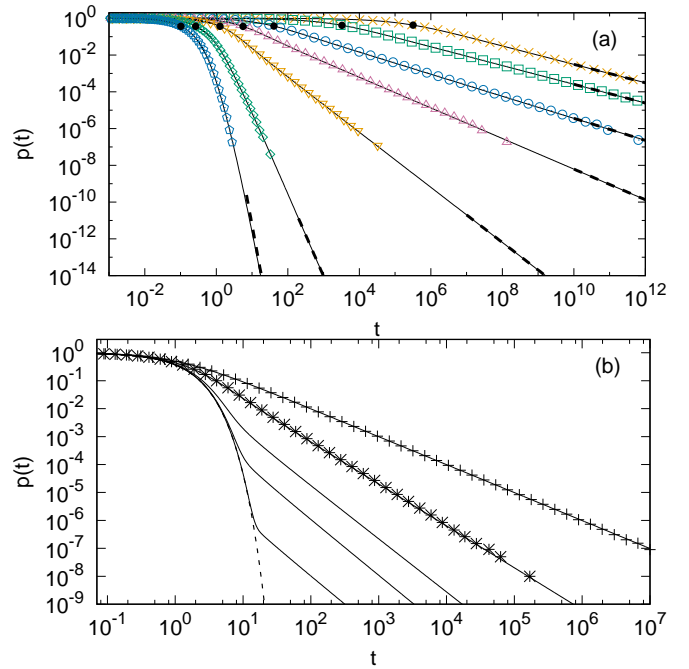


FIG. 3. Survival probability  $p(t)$  for a heavy-tailed  $\psi_\tau(t)$  as in (33) and a reaction-time PDF as in (40) with  $\tau_r = 1$ . (a)  $\alpha = 1/2$ , and (from uppermost to lowermost curve)  $\nu = 10^{-3}, 10^{-2}, 10^{-1}, 1/3, 1, 4, 10$ . (Dashed) Asymptotic form (44). Filled circles indicate the localization time  $\tau_l = \langle\rho^\alpha\rangle^{-1/\alpha}$ . (b)  $\nu = 1$ , with (from uppermost to lowermost curve)  $\alpha = 10^{-3}, 1/2, 0.9, 0.99, 0.9999$ . (dashed)  $\exp(-\langle\rho\rangle t)$ . For both (a) and (b), solid line curves are numerical inversion of (38), symbols are Monte Carlo simulations of the microscopic model.

and leads to segregation. We mentioned above that only in the case  $\langle\tau\rangle = \infty$  does this segregation persist in the scaling limit of vanishing waiting time scale  $\tau_m$ . We now turn our attention to this scenario. We find that the mesoscopic reaction-diffusion equation possesses kernels that couple the independent microscopic physical and chemical fluctuations, which manifest the non-Markovian reaction kinetics. To illustrate, we consider the heavy-tailed waiting time PDF  $\psi_\tau(t)$  that behaves as

$$\psi_\tau(t) \sim \frac{\alpha}{\tau_m \Gamma(1-\alpha)} (t/\tau_m)^{-1-\alpha}, \quad 0 < \alpha < 1, \quad (33)$$

for times larger than the microscopic time scale  $\tau_m$ . Eq. (33) implies that  $\langle\tau\rangle$  diverges. Physically, this corresponds to waiting (or trapping) times that occur on all time scales, including the duration of an experiment. The variation in trapping time may be due to thermal activation over a random binding energy, or to long, slow, excursions in inclusions, or many other causes [35, 36].

The correct scaling limit to employ with (33) is  $\delta \rightarrow 0$  and  $\tau_m \rightarrow 0$  such that

$$\mathcal{D}_\alpha = \delta^2 / (2\tau_m^\alpha) \quad (34)$$

converges to a positive constant. (See Sec. XD.) In this limit, the evolution of the particle density is determined

by the non-Markovian reaction-diffusion equation (See Sec. XD 1.)

$$\begin{aligned} \frac{\partial p(x, t)}{\partial t} - \frac{\partial}{\partial t} \int_0^t dt' K_d(t-t') \mathcal{D}_\alpha \frac{\partial^2 p(x, t')}{\partial x^2} \\ = - \frac{\partial}{\partial t} \int_0^t dt' K_r(t-t') p(x, t'), \end{aligned} \quad (35)$$

where the reaction and diffusion kernels are defined by their Laplace transforms

$$\hat{K}_r(s) = \frac{\langle \rho(s+\rho)^{\alpha-1} \rangle}{s \langle (s+\rho)^{\alpha-1} \rangle}, \quad \hat{K}_d(s) = \frac{1}{s \langle (s+\rho)^{\alpha-1} \rangle}. \quad (36)$$

For  $\rho = 0$ , (36) and (35) reduce to the well-known fractional Fokker-Planck equation. It is worth noting that the operators in (35) describing subdiffusion with random decay rates may be related to fractional calculus via rate-averaged *tempered fractional calculus* [37].

The solution to (35) is (See Sec. XD.)

$$\hat{p}(k, s) = \frac{\langle (s+\rho)^{\alpha-1} \rangle}{\langle (s+\rho)^\alpha \rangle + k^2 \mathcal{D}_\alpha}. \quad (37)$$

We have assumed here that  $p_0(x) = \delta(x)$  for simplicity. The corresponding survival probability obtained by setting  $k = 0$  assumes the compact form

$$\hat{p}(s) = \frac{\langle (s+\rho)^{\alpha-1} \rangle}{\langle (s+\rho)^\alpha \rangle}. \quad (38)$$

Setting  $s = 0$  in (38), we see that the mean survival time  $\langle S \rangle$  of the particle under random diffusion and decay given by (20) takes the form

$$\langle S \rangle = \frac{\langle \rho^{\alpha-1} \rangle}{\langle \rho^\alpha \rangle}. \quad (39)$$

It is important to note that the scaling limit does not exist if the PDF of the rates  $\psi_\rho(r)$  decays more slowly than  $r^{-\alpha-1}$  as  $r \rightarrow \infty$ . In this case the denominator of (39) diverges, so that the mean survival time  $\langle S \rangle = 0$ . Likewise, the kernel  $\hat{K}_r(s)$  in (36) diverges for all  $s$ , and  $\hat{p}(s)$  in (38) is identically zero. Physically,  $\tau_m \rightarrow 0$  means that the rates are sampled very rapidly and for a heavy-tailed rate PDF there is a high probability of very fast rates. On the other hand, if  $\psi_\rho(r)$  diverges more rapidly than  $r^{-\alpha}$  as  $r \rightarrow 0$ , then the numerator of (39) diverges, so that the mean survival time  $\langle S \rangle$  diverges. But, in this case, the scaling limit still exists. For instance, for finite time  $t < \infty$ , (36), (37), and (38) are well defined.

### C. Broadly distributed mean reaction times.

In this section, we focus on rate PDFs that decay as a power-law for  $r$  much smaller than the inverse of the characteristic time  $\tau_r$

$$\psi_\rho(r) \sim \frac{\tau_r \psi_\rho^*(r\tau_r)}{\Gamma(\nu)} (\tau_r r)^{\nu-1}, \quad \nu > 0, \quad (40)$$

where  $\lim_{r \rightarrow 0} \psi_\rho^*(r) = 1$ . This implies a power-law PDF of the mean reaction times  $\psi_r(t) \propto (t/\tau_r)^{-1-\nu}$  for  $t > \tau_r$ . Substituting (40) into (25) we see that the probability to survive decay in a single step varies asymptotically as (See Sec. XD 2.)

$$\Pr(t < \Delta) \sim \left( \frac{t}{\tau_r} \right)^{-\nu}. \quad (41)$$

In general the kernel  $K_r(t)$  approaches the inverse of the mean survival time (39) at a time comparable to the reaction time scale  $\tau_r$ . However, for power law rates (40) and  $\gamma < 1$ , with  $\gamma$  given by (23), computing (39) gives  $\langle S \rangle = \infty$ , and (36) gives  $K_r(t) \sim t^{\gamma-1}$ . In fact, in this case, both kernels (36) take a particularly simple form,  $\hat{K}_r(s) \propto s^{-\gamma}$  and  $\hat{K}_d(s) \propto s^{-\gamma}$ . Thus, for  $\gamma < 1$ , (35) becomes the fractional reaction-diffusion equation (See Sec. XD 3.)

$$\frac{\partial p(x, t)}{\partial t} - \mathcal{D}_\gamma \frac{\partial^{1-\gamma}}{\partial t^{1-\gamma}} \frac{\partial^2 p(x, t)}{\partial x^2} = -k_r \frac{\partial^{1-\gamma}}{\partial t^{1-\gamma}} p(x, t), \quad (42)$$

where  $\mathcal{D}_\gamma \propto \delta^2 / (2\tau_m^\alpha \tau_r^\nu)$  and  $k_r \propto \langle \rho^\alpha \rangle / \tau_r^\nu$ . Although the microscopic reactions are first-order, the macroscopic reaction term in (42) is non-Markovian with a memory kernel that couples the microscopic transport and kinetic parameters. This is made clear in the equation governing the evolution of the survival probability

$$\frac{dp(t)}{dt} = -k_r \frac{\partial^{1-\gamma}}{\partial t^{1-\gamma}} p(t), \quad (43)$$

which is obtained by integrating (42) over  $x$ .

As mentioned earlier, at short times  $t < \tau_r$ , the survival probability is approximately exponential,  $p(t) \approx \exp(-\langle \rho \rangle t)$ . In the case of power-law distributed rates (40) we obtain from (38) the explicit, long time solution (See Sec. XD 2.)

$$p(t) \sim \frac{t^{-\alpha-\nu}}{\tau_r^{-\nu} \langle \rho^\alpha \rangle \Gamma(1-\alpha)}, \quad \tau_m \ll \tau_r \ll t, \quad \nu > 0. \quad (44)$$

Eq. (44) shows that, as anticipated in the definition of the fractional-order derivative of (42), the exponent observed in Fig. 2 is given by  $\gamma = \alpha + \nu$ , which manifests again the intimate coupling of diffusion and reaction mechanisms in the mesoscopic limit. Fig. 3 shows the dependence of  $p(t)$  on  $\alpha$  and  $\nu$ , and the excellent agreement of the derived analytical expressions with Monte-Carlo simulations of the microscopic model. In Sec. XF we give a detailed description of the Monte-Carlo algorithms.

## VI. LOCALIZATION OF PARTICLE DENSITY.

By *localization*, we mean that the surviving-particle density  $p(x, t | t < S)$  approaches a stationary density  $p_s(x) = \lim_{t \rightarrow \infty} p(x, t | t < S)$ . This density has exponential tails and a well-defined, constant, width  $m_s =$



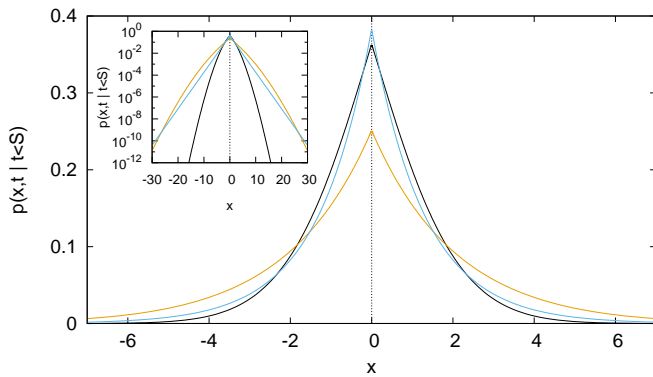


FIG. 4. Density of surviving particles  $p(x, t | t < S)$  with  $\psi_\tau(\tau)$  and  $\psi_\rho(\rho)$  as in Fig. 2, and  $t = 1$  (black),  $t = 8.6$  (yellow),  $t \rightarrow \infty$  (blue). The curve for  $t \rightarrow \infty$  agrees with (45). The inset shows the same curves on a semi-log scale. Curves are numerical inversion of (78).

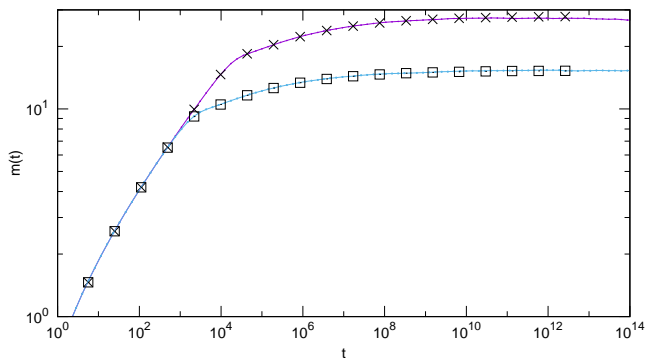


FIG. 5. Mean square displacement  $m(t)$  defined in (11). Symbols are inverse Laplace transform. Lines are stochastic simulations. Heavy-tailed waiting time PDF (33) with  $\alpha = 1/4$ ,  $\tau_m = 0.1$ . Rate PDF (54) with  $p = 1/2$  and (Crosses)  $\tau_r = 10^4$ , (Squares)  $\tau_r = 10^3$ .

$\lim_{t \rightarrow \infty} m(t)$ . Thus, a measurement that detects the local concentration of the surviving species  $A$ , but not that of the product species  $B$ , will be characterized by this width  $m_s$ . Since the surviving-particle density  $p(x, t | t < S)$  ignores the product species  $B$ , it is independent of the fate of  $B$ , which depends on the application. For instance  $B$  may be removed from the system. Or, it may be invisible to the detector but is either immobilized or continues to diffuse. It is interesting to consider the case that species  $B$  is immobile, but it *is* detected along with  $A$ . In this case, the sum of the local concentrations of  $A$  and  $B$  approaches the *same* stationary density  $p_s(x)$  obtained by considering species  $A$  alone [28].

Localization does not occur in the well-mixed case studied in Sec. V A. On the contrary, the decay is spatially uniform. This is evident by first noting that  $p(x, t) = p(t)p_0(x, t)$  satisfies (30) where  $p_0(x, t)$  is the particle density for ordinary diffusion with no decay, i.e.  $\langle \rho \rangle = 0$ . Then referring to (9), we see that this implies  $p(x, t | t < S) = p_0(x, t)$ , which means that the de-

cay is independent of the transport. Finally, substituting this last equality into (11) shows that the MSD  $m(t)$  evolves exactly as in the non-reactive case, increasing without bound. However, in the case of strong chemical and physical fluctuations, when the system remains poorly-mixed, the particles are localized at long times. The surviving-particle density tends to a stationary state  $p_s(x) \equiv \lim_{t \rightarrow \infty} p(x, t | t < S)$ , given by (See Sec. X D.)

$$p_s(x) = \frac{1}{2l} e^{-|x|/l}, \quad (45)$$

where the *localization time*  $\tau_l$  and *localization length*  $l$  are given by

$$\tau_l = \langle \rho^\alpha \rangle^{-1/\alpha} \quad \text{and} \quad l = \sqrt{D_\alpha \tau_l^\alpha}. \quad (46)$$

The corresponding MSD approaches a constant value given by

$$m_s = \lim_{t \rightarrow \infty} m(t) = 2D_\alpha \tau_l^\alpha = 2l^2.$$

This localization is clearly verified and illustrated in both the MSD  $m(t)$  in Fig. 2 and Fig. 5, and the particle density in Fig. 4. The MSD approaches a constant at long times. As  $t \rightarrow \infty$ , the density of surviving particles approaches (45) which is represented by the blue curve in Fig. 4. Note that the localization time  $\tau_l$  marks the scale at which the mean square displacement crosses over from the power-law behavior  $m(t) \propto t^\alpha$  to the constant value, as illustrated in Fig. 2. The deviation of  $m(t)$  from a power-law for  $t < \tau_r$  in Fig. 5 is due to corrections to the scaling limit. See Sec. X F for details of the numerical methods.

To recap, we have derived the fractional reaction-diffusion equations (35), (42) and fractional kinetic equation (43) in the scaling limit of the random walk. These are exact solutions of the microscopic model with no homogenization or upscaling. The presence of memory kernels coupling the transport and kinetic parameters manifests the poor mixing, even in the scaling limit, in contrast to the perfect mixing in the scaling limit for Brownian diffusion (30). We have derived exact expressions in the scaling limit for the particle density (37) and survival probability (38). We presented the asymptotic solutions for the survival probability (44) and for the localized (stationary) particle density (45) and (46). These derivations and their physical interpretation are the main results of Sec. V and Sec. VI.

## VII. COUPLED VS. UNCOUPLED REACTION.

To better understand stochastic decay, it is useful to compare the mesoscopic description of the random decay model to that of other models of reaction-subdiffusion. We refer to a model in which the reaction proceeds independently of the transport as “uncoupled”. Otherwise,

it is “coupled”. The question of whether a model is coupled or uncoupled is an instructive point of comparison, which we address in the following.

### A. Uncoupled reaction

Suppose  $P(x, t)$  is the density of surviving particles undergoing subdiffusion and an unspecified decay process. Define  $q(x, t)$  via

$$q(x, t) \equiv \frac{P(x, t)}{p_0(x, t)}, \quad (47)$$

where  $p_0(x, t)$  is a solution to the fractional Fokker-Planck equation with no decay [38]

$$\frac{\partial p_0(x, t)}{\partial t} = K_\alpha D_t^{1-\alpha} \frac{\partial^2}{\partial x^2} p_0(x, t), \quad (48)$$

and  $D_t^{1-\alpha}$  is the Riemann-Liouville fractional derivative [38]. Substituting  $p_0(x, t) = P(x, t)/q(x, t)$  into (48) we see that  $P(x, t)$  satisfies the equation

$$\frac{\partial P(x, t)}{\partial t} = q(x, t) K_\alpha D_t^{1-\alpha} \frac{\partial^2}{\partial x^2} \left[ \frac{P(x, t)}{q(x, t)} \right] + \frac{\partial_t q(x, t)}{q(x, t)} P(x, t). \quad (49)$$

By construction, (49) holds formally for any density  $P(x, t)$ , with  $q(x, t)$  given by (47). But it is evidently only meaningful if  $P(x, t)$  results from a particle that diffuses according to (48), and is subject to decay that is *independent* of the dynamics [22, 39–43]. This becomes clear upon considering the time rate of change of mass at position  $x$  and time  $t$

$$\frac{\partial_t P(x, t)}{P(x, t)}. \quad (50)$$

Using (47) we write (50) as

$$\frac{\partial_t P(x, t)}{P(x, t)} = \frac{\partial_t p_0(x, t)}{p_0(x, t)} + \frac{\partial_t q(x, t)}{q(x, t)}. \quad (51)$$

The first term on the right hand side is the rate due to transport. We are interested in the second term  $[\partial_t q(x, t)]/q(x, t)$ , which is the instantaneous decay rate (times  $-1$ ) at position  $x$ . The role of the second term as a time and space dependent decay rate is also clear in the last term in (49). The diffusion and decay in (51) are manifestly independent. It is important to note that the reaction term in (49) is Markovian, that is, local in time. Indeed, integrating (49) over space, we find an equation for the survival probability

$$\frac{\partial P(t)}{\partial t} = \int_{-\infty}^{\infty} dx \frac{\partial_t q(x, t)}{q(x, t)} P(x, t). \quad (52)$$

If we allow  $q(x, t)$  to depend on the density  $P(x, t)$  itself, then (52) is non-linear [41]. Still, the decay is independent of the dynamics and is Markovian. Eq. (49)

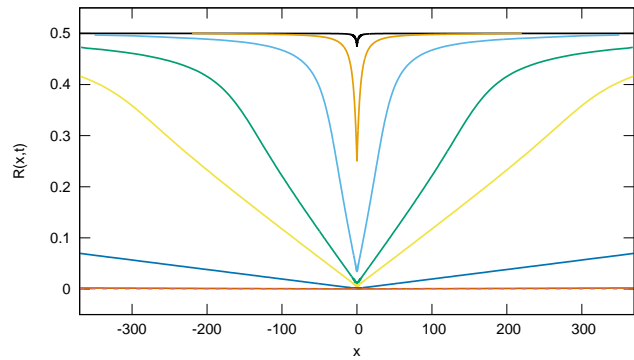


FIG. 6. Decay rate  $R(x, t)$  defined in (53). Times from uppermost to lowermost curve (black, gold, light blue, green, yellow, dark blue, orange):  $t = 0.6, 7, 42, 136, 246, 1450, 5 \times 10^4$ . Waiting time PDF (33),  $\alpha = 0.7$ , Decay rate PDF (97),  $\tau_r = 1$ ,  $\nu = 1$ . Scaling limit with generalized diffusivity  $\mathcal{D}_\alpha = 1$ .

has been derived for many models of uncoupled dynamics and decay, appearing, for example, as Eq. (20) in Ref. [22], Eq. (29) in Ref. [40], and Eq. (23) in Ref. [41]. Typically,  $q(x, t)$  is independent of  $P(x, t)$ , so that any  $x$ -dependence in  $q(x, t)$  represents independent, externally imposed, spatially varying decay.

### B. Coupled reaction

The random decay model strongly couples chemical kinetics and transport, which results in a very different description and behavior. There is no explicit space-dependent decay in the microscopic model of Sec. II B as there is in (49). However the strong coupling results in a non-Markovian reaction term in (35) and in (42), which in turn gives rise to a time- and space-dependent decay rate  $R(x, t)$ . The decay rate  $R(x, t)$  is that part of the time rate of change of the density  $p(x, t)$  that is not due to transport. It is an *effective* or *mesoscale* rate that emerges from microscopic kinetics and transport that have no explicit space dependence.

To compute  $R(x, t)$  for the random rate model, we begin by dividing (35) by  $p(x, t)$ , thereby obtaining an expression for the time rate of change of the mass that is analogous to the expression for independent decay (51). Then  $R(x, t)$  is given by the last term in (35) divided by  $p(x, t)$ ,

$$R(x, t) = [p(x, t)]^{-1} \frac{\partial}{\partial t} \int_0^t dt' K_r(t-t') p(x, t'). \quad (53)$$

$R(x, t)$  depends on the history of the particle density at  $x$  through the kernel  $K_r(t)$ . Thus, it is the non-Markovian operator that induces a spatial dependence in the effective decay rate. The solution to (53) by numerical inversion of the Laplace transform is shown in Fig. 6. At

short times  $t \ll \tau_r$ , the decay is uniform and exponential with rate  $\langle \rho \rangle = 1/2$ . This corresponds to the dotted line in Fig. 2. At intermediate times, Fig. 6 clearly shows a strongly inhomogeneous decay rate. Because  $p(t)$  decays as a power at long times, the instantaneous decay rate averaged over space  $[\partial_t p(t)]/p(t)$  decreases like  $t^{-1}$ . As  $t$  increases, the decay rate near  $x = 0$  approaches zero, but the asymptotic value as  $x$  approaches  $\pm\infty$  is  $\langle \rho \rangle$ . This suppression of the decay rate in the central part of the density is responsible for the localization discussed in Sec. VI.

Another case of coupling transport and decay is that in which the walker does not decay while waiting, but rather only before or after making a step [43–45]. Suppose a fraction  $p$  of walkers are removed at the beginning of each waiting period. Compare this to the random decay model with rate density

$$\psi_\rho(r) = (1 - p)\delta(r) + p\delta(r - \tau_r^{-1}), \quad (54)$$

which means that during each waiting period the walker suffers no decay with probability  $1 - p$  and decays at rate  $1/\tau_r$  with probability  $p$ . It can be shown that (42) holds in this case with  $\nu = 0$ . For times  $t \gg \tau_r$ , the longest trapping times are important, so that the particle decays very early in the waiting period. This is equivalent to removing the walker with probability  $p$  at the beginning of the step. The fractional reaction-diffusion equation for the latter model given in Ref. [44] is indeed equal to (42) with  $\nu = 0$ .

### VIII. LOWER CUT-OFF IN RATE PDF.

Thus far, we have considered rate distributions with rates arbitrarily close to zero. But, suppose we shift  $\rho$ , that is, let  $\rho \rightarrow \rho + r_c$  with  $r_c > 0$  so that the probability that  $r < r_c$  is zero. We show in Appendix XC 2 that the propagator  $p_c(x, t)$  for the shifted reaction rates is

$$p_c(x, t) = \exp(-r_c t)p(x, t), \quad (55)$$

where  $p(x, t)$  is the solution for the unshifted density  $\psi_\rho(r)$ . Note that this leaves  $p(x, t|t < S)$  unchanged, so that  $p_c(x, t)$  shows the same localization as  $p(x, t)$ . However, the asymptotic survival probability (44) now decays exponentially fast with the *smallest* rate  $r_c$ . For instance, for the power law  $\psi_\rho(r)$  (40) and  $r_c \ll r_0$  the survival probability follows the truncated power law  $p_c(t) \propto \exp(-r_c t)t^{-\alpha-\nu}$ .

### IX. CONCLUSIONS AND OUTLOOK

We derived the mesoscale behavior of a reaction-diffusion system characterized by microscopically fluctuating transport and reaction kinetics, using the framework of a continuous time random walk that samples disordered decay rates. We showed that broadly distributed

waiting and reaction times give rise in the scaling limit to a generalized fractional reaction-diffusion equation with non-Markovian reaction and diffusion operators both of which are characterized by intimate coupling of microscopic chemical and physical parameters. This equation describes a system that asymptotically remains poorly mixed leading to power-law kinetics and spatially inhomogeneous reactions. The resulting decay is manifest in a particle density whose profile differs radically from that given by nonreactive subdiffusive CTRW, most notably in a stationary (localized) particle density at long times. This is in stark contrast to the case of ordinary diffusion in the scaling limit, which experiences spatially uniform decay with a rate equal to the average of the disordered rates.

Understanding of the mechanisms by which mesoscale behavior emerges from microscopic disorder plays a key role in diverse physical systems. For example, observed scale effects in reaction laws and decrease in reactivity on large scales in geological media [23, 24, 46] can be attributed to spatial heterogeneity in the chemical and physical medium properties. Sometimes these behaviors are modeled by empirical non-linear reaction rate laws [47]. Our results show that physical and chemical system fluctuations are unambiguously attributable to non-Markovian, but linear kinetics. The segregation of reactions, here a mobile and an immobile species, in the presence of fluctuating chemical properties, leads to a broad distribution of effective reaction time scales, which are composed of both transport and reaction times. The reaction process itself is history dependent, as expressed by the non-local kinetic rate law (18). This new understanding of the role of chemical and physical fluctuations provides a systematic way towards quantifying effective large scale reaction behaviors and scale effects in reactivity in terms of the physical and chemical heterogeneity of the host medium in natural and engineered media. Furthermore, the results derived for first-order decay can be generalized to more complex chemical reactions under stochastic reaction and transport rates along the lines of the approach presented in [48].

We have focused on transport in the presence of random translation times and decay rates. However, it is important to point out that the theory presented here is independent of the specific physical context in which it was developed. We derived the main results for a general stochastic framework that combines two processes, CTRW and first passage under restart, by identifying the CTRW waiting time with the restart time. Applications and mathematical properties of CTRW [36, 49] and first passage time (FPT) under restart [29, 32] have been studied intensively. But the fruitful union of these two theories remains nearly unexplored. Possible avenues can be found in the many diverse processes that determine statistics of the step displacement  $\xi$  [50, 51], waiting time  $\tau$  [3–5], and single-step decay time  $\Delta$  [8].

However, an important class of chemical processes, namely Michaelis-Menten (MM) reactions [52], require

further generalization of FPT under reset. In recent years, advances in single-molecule spectroscopy have opened the possibility of measuring and controlling [53] catalysis on the level of single, or a few, molecules. This in turn has spurred the development of stochastic approaches to MM reactions. These include considering the effects of fluctuations [54, 55], internal states of the enzyme [56], and non-Poissonian processes. A stochastic Michaelis-Menten scheme is obtained from the generic FPT under reset by delaying restart of the process by a random time  $T_{\text{on}}$  after each interruption. In catalytic reactions,  $T_{\text{on}}$  represents the rebinding time. In this stochastic formulation, recent theoretical studies have predicted experimentally accessible [57], counter-intuitive kinetics by replacing the classical Poissonian processes governing binding, unbinding, and catalysis times with non-Poissonian processes [58–60]. The importance of extending this Michaelis-Menten scheme to include heterogeneous catalysis due to a fluctuating environment has been recognized in recent experimental [61] and theoretical [59] work. An attractive possibility is to modify the framework presented herein by including the rebinding time  $T_{\text{on}}$ . This immediately yields a Michaelis-Menten scheme capable of handling heterogeneous catalysis via diffusion following unbinding events. The challenge of understanding the interplay of transport and Michaelis-Menten-like processes in cellular environments [9, 59] is a particularly promising candidate for such a Michaelis-Menten-CTRW approach, given that macromolecular crowding in cells may lead to both CTRW-like subdiffusion [36, 62] and modified binding dynamics [63–65].

## X. APPENDIX

### A. Derivation of the integral equations for the propagator

Here we derive (12) from the microscopic model given in Sec. II. The assumption of an unbiased walk with finite step variance [See (6) and (72).], will be employed when passing to the scaling limit, but does not enter here. The particle density (9) may be written

$$p(x, t) = \left\langle \delta(x - x_{n_t}) \mathbb{I}(t < S) \right\rangle.$$

Recall that the indicator function  $\mathbb{I}(\cdot)$  is 1 if the argument is true and 0 otherwise. The factor  $\mathbb{I}(t < S)$  may be decomposed as follows. From the transition rules (3) and (5) it follows that, at a given time  $t$ , a particle that is at position  $x_n$  has survived until the turning time  $t_n$  with probability  $\left\langle \prod_{i=0}^{n_t-1} \mathbb{I}(\tau_i < \Delta_i) \right\rangle$ , and has survived the last time interval  $(t - t_n)$  from the last turning point to the present time with probability  $\langle \mathbb{I}(t - t_{n_t} < \Delta_{n_t}) \rangle$ . Referring to (4), this implies that the particle density at

time  $t$  is given by

$$p(x, t) = \left\langle \delta(x - x_{n_t}) \prod_{i=0}^{n_t-1} \mathbb{I}(\tau_i < \Delta_i) \mathbb{I}(t - t_{n_t} < \Delta_{n_t}) \right\rangle,$$

where the random variable  $n_t = \max(n | t_n \leq t)$  is the number of steps performed up to time  $t$ . We partition the probability space into disjoint sets, so that the expectation becomes a sum of expectations

$$p(x, t) = \sum_{n=0}^{\infty} \left\langle \delta(x - x_n) \prod_{i=0}^{n-1} \mathbb{I}(\tau_i < \Delta_i) \mathbb{I}(t - t_n < \min[\tau_n, \Delta_n]) \right\rangle$$

The last factor combines the requirements that particle has neither decayed nor jumped during the increment  $t - t_n$ . We now separate explicitly the contributions up to the last turning point at time  $t'$  and during the final resting interval  $t - t'$

$$p(x, t) = \int_0^t dt' \sum_{n=0}^{\infty} \left\langle \delta(x - x_n) \delta(t' - t_n) \times \prod_{i=0}^{n-1} \mathbb{I}(\tau_i < \Delta_i) \mathbb{I}(t - t' < \min[\tau_n, \Delta_n]) \right\rangle.$$

Because the last factor depends only on  $\tau_n$  and  $\Delta_n$ , which are independent of the remaining factors, we split the expectation into two factors obtaining

$$p(x, t) = \int_0^t dt' \sum_{n=0}^{\infty} \left\langle \delta(x - x_n) \delta(t' - t_n) \right\rangle \Pr(t - t' < \min[\tau, \Delta]), \quad (56)$$

$$\times \prod_{i=0}^{n-1} \mathbb{I}(\tau_i < \Delta_i) \quad (57)$$

where we have also used the fact that the step variables share a common distribution. We now define

$$\eta_n(x, t) = \left\langle \delta(x - x_n) \delta(t - t_n) \prod_{i=0}^{n-1} \mathbb{I}(\tau_i < \Delta_i) \right\rangle, \quad (58)$$

and

$$\eta(x, t) = \sum_{n=0}^{\infty} \eta_n(x, t).$$

Eq. (58) denotes the joint probability density for a particle to arrive at position  $x$  at time  $t$  on the  $n$ th step. With these definitions, (56) is rewritten

$$p(x, t) = \int_0^t dt' \eta(x, t') \Pr(t - t' < \min[\tau, \Delta]) \quad (59)$$



We analyze  $\eta_n(x, t)$  by writing  $\eta_{n+1}(x, t)$  in the following form

$$\begin{aligned} \eta_{n+1}(x, t) &= \int_{-\infty}^{\infty} dx' \int_0^t dt' \langle \delta(x' - x_n) \delta(t' - t_n) \\ &\times \prod_{i=0}^{n-1} \mathbb{I}(\tau_i < \Delta_i) \delta(x - x' - \xi_n) \delta(t - t' - \tau_n) \\ &\times \mathbb{I}(\tau_n < \Delta_n) \rangle. \end{aligned}$$

That this is indeed the expression for  $\eta_{n+1}(x, t)$  can be seen by performing the integrals and eliminating either one of the delta functions for  $x'$  and either one for  $t'$ , and using (3). Note that the only random variables appearing in the last three factors in the expectation are  $\xi_n$ ,  $\tau_n$  and  $\Delta_n$ , while the first three factors depend only on random variables for  $i < n$ . The last three factors are thus independent of the first three and we can again factor the expectation. Furthermore, per the Dirac delta  $\delta(t - t' - \tau_n)$ , we have  $\tau_n = t - t'$ . Thus, we can write

$$\begin{aligned} \eta_{n+1}(x, t) &= \int_{-\infty}^{\infty} dx' \int_0^t dt' \\ &\left\langle \delta(x' - x_n) \delta(t' - t_n) \prod_{i=0}^{n-1} \mathbb{I}(\tau_i < \Delta_i) \right\rangle \\ &\times \langle \delta(x - x' - \xi_n) \rangle \langle \delta(t - t' - \tau_n) \mathbb{I}(\tau_n < \Delta_n) \rangle. \end{aligned}$$

Now, referring to (58), we identify the first factor in angular brackets with  $\eta_n(x', t')$ , the second factor with  $\psi_\xi(x - x')$  and the third factor with  $\phi_{\tau\Delta}(t - t')$ . Thus, we obtain

$$\begin{aligned} \eta_{n+1}(x, t) &= \int_{-\infty}^{\infty} dx' \int_0^t dt' \psi_\xi(x - x') \\ &\times \phi_{\tau\Delta}(t - t') \eta_n(x', t'). \end{aligned} \quad (60)$$

Summation over  $n$  from 0 to infinity on both sides of (60) gives for  $\eta(x, t)$

$$\begin{aligned} \eta(x, t) &= p_0(x) \delta(t) + \int_{-\infty}^{\infty} dx' \int_0^{\infty} dt' \eta(x', t') \\ &\times \psi_\xi(x - x') \phi_{\tau\Delta}(t - t'), \end{aligned} \quad (61)$$

where we have used

$$\sum_{n=0}^{\infty} \eta_{n+1}(x, t) = \sum_{n=0}^{\infty} \eta_n(x, t) - \eta_0(x, t). \quad (62)$$

Integral equations (59) and (61), appear in the main body of the paper as (12).

## B. Derivation of the generalized Master equation

We derive the generalized Master equation (16). To this end, we Laplace transform (59) and (61), which gives

$$\hat{p}(x, s) = \hat{\eta}(x, s) \hat{\Phi}_{\tau\Delta}(s) \quad (63)$$

$$\hat{\eta}(x, s) = p_0(x) + \int_{-\infty}^{\infty} dx' \hat{\eta}(x', s) \tilde{\psi}_\xi(x - x') \hat{\phi}_{\tau\Delta}(s). \quad (64)$$

We now solve (63) for  $\hat{\eta}(x, s)$  and insert it into (64) to obtain

$$\begin{aligned} \hat{p}(x, s) \frac{1}{\hat{\Phi}_{\tau\Delta}(s)} &= p_0(x) \\ &+ \int_{-\infty}^{\infty} dx' \hat{p}(x', s) \frac{\hat{\phi}_{\tau\Delta}(s)}{\hat{\Phi}_{\tau\Delta}(s)} \psi_\xi(x - x'). \end{aligned} \quad (65)$$

We now rewrite the left hand side tautologically as

$$\begin{aligned} s\hat{p}(x, s) + \hat{p}(x, s) \left[ \frac{1}{\hat{\Phi}_{\tau\Delta}(s)} - s \right] \\ = s\hat{p}(x, s) + \hat{p}(x, s) \left[ \frac{1 - s\hat{\Phi}_{\tau\Delta}(s)}{\hat{\Phi}_{\tau\Delta}(s)} \right] \end{aligned}$$

Using  $-\partial_t \Phi_{\tau\Delta}(t) = \phi_{\tau\Delta}(t) + \phi_{\Delta\tau}(t)$  [See (14).] we rewrite the numerator, obtaining

$$s\hat{p}(x, s) + \hat{p}(x, s) \left[ \frac{\hat{\phi}_{\tau\Delta}(s) + \hat{\phi}_{\Delta\tau}(s)}{\hat{\Phi}_{\tau\Delta}(s)} \right]$$

Replacing the left hand side of (65) with the last expression and rearranging, we obtain

$$\begin{aligned} s\hat{p}(x, s) - p_0(x) &= -\hat{p}(x, s) \frac{\hat{\phi}_{\Delta\tau}(s)}{\hat{\Phi}_{\tau\Delta}(s)} \\ &+ \int_{-\infty}^{\infty} dx' [\hat{p}(x', s) - p(x, s)] \frac{\hat{\phi}_{\tau\Delta}(s)}{\hat{\Phi}_{\tau\Delta}(s)} \psi_\xi(x - x'). \end{aligned} \quad (66)$$

Inverse Laplace transform of the last equation gives the generalized Master equation (16) with kernels defined via (17) in the main body of the paper.

## C. Fourier-Laplace solutions

### 1. Generalized Montroll-Weiss equation

Taking the Fourier transform of (63) and (64) we obtain

$$\hat{\hat{p}}(k, s) = \hat{\hat{\eta}}(k, s) \hat{\hat{\Phi}}_{\tau\Delta}(s) \quad (67)$$

$$\hat{\hat{\eta}}(k, s) = \tilde{p}_0(k) + \hat{\hat{\eta}}(k, s) \tilde{\psi}_\xi(k) \hat{\hat{\phi}}_{\tau\Delta}(s). \quad (68)$$

Solving (68) for  $\hat{\eta}(k, s)$  and substituting the solution into (67), we obtain the generalized Montroll-Weiss equation (19).

### 2. Shift of the random reaction rate by a constant $r_c$

We consider the effect of shifting the random reaction rate  $\rho \rightarrow r_c + \rho$ . Inserting this shift into (27) gives

$$\hat{p}_c(k, s) = \frac{\tilde{p}_0(k) \langle \hat{\Psi}_\tau(s + \rho + r_c) \rangle}{1 - \tilde{\psi}_\xi(k) \langle \hat{\psi}_\tau(s + \rho + r_c) \rangle}.$$

Inverse Fourier-Laplace transform gives, by using the shift theorem of the Laplace transform

$$p_c(x, t) = \exp(-r_c t) p(x, t)$$

Integrating over  $x$  gives

$$p_c(t) = \exp(-r_c t) p(t),$$

where  $p(x, t)$  and  $p(t)$  are propagator and survival probability for  $r_c = 0$ . This derives (55).

### 3. Mean square displacement

The mean square displacement of the surviving particles is given by

$$\begin{aligned} m(t) &= - \left. \frac{\partial^2 \ln \tilde{p}(k, t)}{\partial k^2} \right|_{k=0} \\ &= - \tilde{p}(0, t)^{-1} \left. \frac{\partial^2 \tilde{p}(k, t)}{\partial k^2} \right|_{k=0}. \end{aligned} \quad (69)$$

Under the assumption  $p_0(x) = \delta(x)$  and that the moments of the random displacement  $\xi$  satisfy (6), we obtain from (27) the explicit Laplace-space expression

$$- \left. \frac{\partial^2 \hat{p}(k, s)}{\partial k^2} \right|_{k=0} = \frac{\delta^2 \langle \frac{1 - \hat{\psi}_\tau(s + \rho)}{s + \rho} \rangle \langle \hat{\psi}_\tau(s + \rho) \rangle}{(1 - \langle \hat{\psi}_\tau(s + \rho) \rangle)^2}. \quad (70)$$

We obtain the Laplace transform of the moments  $\langle x(t)^n \rangle$  in the scaling regime directly from (37) as

$$\begin{aligned} (-i)^n \left. \frac{\partial^n \hat{p}(k, s)}{\partial k^n} \right|_{k=0} &= n! \mathcal{D}_\alpha^{\frac{n}{2}} \hat{p}(s) [ \langle (s + \rho)^\alpha \rangle ]^{-\frac{n}{2}}, \\ &n = 0, 2, 4, \dots \end{aligned} \quad (71)$$

### D. Scaling limit

We first consider the case  $\langle \tau \rangle < \infty$ . This implies the Laplace transform of  $\psi_\tau(t)$  is  $\hat{\psi}_\tau(s) = 1 - s\tau_m + o(\tau_m)g(s)$ . And from (6) the Fourier transform of the step PDF is

$$\tilde{\psi}_\xi(k) = 1 - \frac{(\delta k)^2}{2} + o(\delta^2)h(k). \quad (72)$$

The “o” notation means  $\lim_{\tau_m \rightarrow 0} o(\tau_m)/\tau_m = 0$  and  $\lim_{\delta \rightarrow 0} o(\delta^2)/\delta^2 = 0$ . In Fourier-Laplace space, the particle density  $p(x, t|t < S)$  is given by (27)

$$\hat{p}(k, s) = \frac{\langle \hat{\Psi}_\tau(s + \rho) \rangle}{1 - \tilde{\psi}_\xi(k) \langle \hat{\psi}_\tau(s + \rho) \rangle}, \quad (73)$$

where we take  $p_0(x) = \delta(x)$  for convenience. Using the expansions of the PDFs and noting that (26) implies  $\hat{\Psi}_\tau(s) = [1 - \hat{\psi}_\tau(s)]/s$ , we have

$$\hat{p}(k, s) = \frac{\tau_m + o(\tau_m) \langle \frac{g(s + \rho)}{s + \rho} \rangle}{\frac{k^2 \delta^2}{2} + \tau_m \langle s + \rho \rangle + o(\delta^2)h(k) + o(\tau_m) \langle g(s + \rho) \rangle}. \quad (74)$$

Dividing numerator and denominator by  $\tau_m$  and taking the scaling limit  $\delta \rightarrow 0$  and  $\tau_m \rightarrow 0$  such that

$$\mathcal{D} = \delta^2 / (2\tau_m)$$

is a positive constant, (74) becomes

$$\hat{p}(k, s) = \frac{1}{\frac{k^2 \delta^2}{2\tau_m} + s + \langle \rho \rangle}. \quad (75)$$

Eq. (75) is the Fourier-Laplace transform of the propagator for Brownian motion with no reactions, with  $s$  replaced by  $s + \langle \rho \rangle$ . Thus, the solution is  $p(x, t) = \exp(-\langle \rho \rangle t) p_0(x, t)$ .

For the waiting time PDF (33), we have  $\langle \tau \rangle < \infty$ . Thus, the Laplace transform of  $\psi_\tau(t)$  is  $\hat{\psi}_\tau(s) = 1 - (s\tau_m)^\alpha + o(\tau_m^\alpha)g(s)$ . Together with (72), this yields the joint PDF  $\hat{\psi}(k, s) = 1 - \delta^2 k^2 / 2 - (s\tau_m)^\alpha + o(\tau_m^\alpha)g(s) + o(\delta^2)h(k)$ . Substituting these asymptotic forms into (73), we find

$$\hat{p}(k, s) = \frac{\tau_m^\alpha \langle (s + \rho)^{\alpha-1} \rangle + o(\tau_m^\alpha) \langle \frac{g(s + \rho)}{s + \rho} \rangle}{\frac{k^2 \delta^2}{2} + \tau_m^\alpha \langle (s + \rho)^\alpha \rangle + o(\delta^2)h(k) + o(\tau_m^\alpha) \langle g(s + \rho) \rangle}. \quad (76)$$

Dividing by  $\tau_m^\alpha$  and taking the limit  $\delta \rightarrow 0$  and  $\tau_m \rightarrow 0$  such that

$$\mathcal{D}_\alpha = \delta^2 / (2\tau_m^\alpha)$$

converges to a positive constant, we obtain

$$\hat{p}(k, s) = \frac{\langle (s + \rho)^{\alpha-1} \rangle}{\langle (s + \rho)^\alpha \rangle + k^2 \mathcal{D}_\alpha}, \quad (77)$$

which is (37).

The inverse Fourier transform of (77) yields the propagator in Laplace space

$$\hat{p}(x, s) = \frac{\hat{p}(s)}{2} \mathcal{R}(s) e^{-|x|\mathcal{R}(s)}, \quad (78)$$

where  $\mathcal{R}(s) \equiv \mathcal{D}_\alpha^{-1/2} \langle (s + \rho)^\alpha \rangle^{1/2}$ . As  $s \rightarrow 0$  the inverse Laplace transform of (78) is dominated by the factor  $\hat{p}(s)$  so that  $\hat{p}(x, s)$  can be approximated by

$$\hat{p}(x, s) \approx \hat{p}(s) \frac{\mathcal{R}(0)}{2} e^{-|x|\mathcal{R}(0)} \quad (79)$$

Taking the inverse Laplace transform and dividing by  $p(t)$  we obtain the stationary density  $p_s(x)$  in (45). On the other hand, for  $t < \tau_r$ , the survival probability is approximately exponential and thus the propagator  $p(x, t) \approx \exp(-(\rho)t)p_0(x, t)$ , where  $p_0(x, t)$  is the density for non-reactive particles obtained by setting  $\rho = 0$  in (78).

### 1. Derivation of generalized fractional reaction diffusion equation

We begin with the generalized Montroll-Weiss equation (37), but include the general initial particle density  $p_0(x)$ .

$$\hat{p}(k, s) = \frac{\tilde{p}_0(k) \langle (s + \rho)^{\alpha-1} \rangle}{\langle (s + \rho)^\alpha \rangle + k^2 \mathcal{D}_\alpha}.$$

Multiplying by the denominator, we have

$$\begin{aligned} \hat{p}(k, s) \langle (s + \rho)^\alpha \rangle \\ = -\mathcal{D}_\alpha k^2 \hat{p}(k, s) + \tilde{p}_0(k) \langle (s + \rho)^{\alpha-1} \rangle \end{aligned} \quad (80)$$

We rewrite the factor on the left hand side as

$$\langle (s + \rho)^\alpha \rangle = s \langle (s + \rho)^{\alpha-1} \rangle + \langle \rho(s + \rho)^{\alpha-1} \rangle,$$

and divide the equation by  $s \langle (s + \rho)^{\alpha-1} \rangle$  to obtain

$$\begin{aligned} \hat{p}(k, s) + \hat{p}(k, s) \frac{\langle \rho(s + \rho)^{\alpha-1} \rangle}{s \langle (s + \rho)^{\alpha-1} \rangle} \\ = -\mathcal{D}_\alpha k^2 \frac{1}{s \langle (s + \rho)^{\alpha-1} \rangle} + \frac{\tilde{p}_0(k)}{s}. \end{aligned} \quad (81)$$

This can be written

$$\begin{aligned} \hat{p}(k, s) + \hat{K}_r(s) \hat{p}(k, s) \\ = -\mathcal{D}_\alpha k^2 \hat{K}_d(s) \hat{p}(k, s) + \frac{\tilde{p}_0(k)}{s}. \end{aligned} \quad (82)$$

where  $K_r(s)$  and  $K_d(s)$  are given by (36). Inverting we obtain

$$\begin{aligned} p(x, t) - \int_0^t dt' K_d(t - t') \mathcal{D}_\alpha \frac{\partial^2 p(x, t')}{\partial x^2} \\ = - \int_0^t dt' K_r(t - t') p(x, t') + p_0(x). \end{aligned} \quad (83)$$

Taking the derivative of (83) gives (35).

### 2. Asymptotic form of $p(t)$

The expression for the survival probability in the scaling limit is (38)

$$\hat{p}(s) = \frac{\langle (s + \rho)^{\alpha-1} \rangle}{\langle (s + \rho)^\alpha \rangle}. \quad (84)$$

We begin with the numerator. Exchanging the order of the integrals, we have

$$\mathcal{L}^{-1} \{ \langle (s + \rho)^{\alpha-1} \rangle \} = \langle \mathcal{L}^{-1} \{ s^{\alpha-1} \} e^{-\rho t} \rangle,$$

from which we obtain

$$\mathcal{L}^{-1} \{ \langle (s + \rho)^{\alpha-1} \rangle \} = \frac{t^{-\alpha}}{\Gamma(1 - \alpha)} \langle e^{-\rho t} \rangle. \quad (85)$$

It is easy to show that the numerator in (84) is more singular than the denominator for  $s \rightarrow 0$ . This can be seen, for instance, by taking derivatives until the leading order term diverges as  $s \rightarrow 0$ . So, we can set  $s = 0$  in the denominator to find

$$p(t) \sim \frac{t^{-\alpha} \langle e^{-\rho t} \rangle}{\langle \rho^\alpha \rangle \Gamma(1 - \alpha)}.$$

Using the density (40), we have

$$\langle e^{-\rho t} \rangle = \frac{\tau_r^\nu}{\Gamma(\nu)} \int_0^\infty e^{-tr} r^{\nu-1} \psi_\rho^*(\tau_r r) dr \quad (86)$$

Substituting  $z = tr$ , we find for  $t \gg \tau_r$

$$\langle e^{-\rho t} \rangle \sim \left( \frac{t}{\tau_r} \right)^{-\nu}. \quad (87)$$

Substituting (87) into (86), we find

$$p(t) \sim \frac{t^{-\alpha-\nu}}{\tau_r^{-\nu} \langle \rho^\alpha \rangle \Gamma(1 - \alpha)}, \quad \nu > 0,$$

which is Eq. (44) in the main text.

### 3. Fractional reaction-diffusion equation

We now show that using the power-law rate PDF (40) and assuming  $0 < \alpha + \nu < 1$ , the operators in (35) reduce to standard Liouville fractional derivatives, which lead to a fractional reaction-diffusion equation. Although the equation involves only the standard Liouville fractional derivatives, the order of the derivative depends on *both* reaction and transport exponents. The fractional nature of the kernels comes from their asymptotic divergence as  $s \rightarrow 0$ . We begin by analyzing the denominator of the kernels (36)  $s \langle (s + \rho)^{\alpha-1} \rangle$ . Using the rate density (40), the second factor becomes

$$\begin{aligned} \langle (s + \rho)^{\alpha-1} \rangle &\sim \frac{\tau_r^\nu}{\Gamma(\nu)} \int_0^\infty (s + r)^{\alpha-1} r^{\nu-1} \psi_\rho^*(r \tau_r) dr \\ &= \frac{s^{\alpha+\nu-1}}{\tau_r^{-\nu} \Gamma(\nu)} \int_0^\infty (1 + z)^{\alpha-1} z^{\nu-1} \psi_\rho^*(sz \tau_r) dz, \end{aligned}$$

where we have made the substitution  $r = sz$ .

For  $s \tau_r \ll 1$ , the last integral converges while the factor  $\psi_\rho^*(sz \tau_r)$  remains near 1. But, the prefactor  $s^{\alpha+\nu-1}$

diverges. Replacing  $\psi_\rho^*(sz\tau_r)$  by  $\psi_\rho^*(0) = 1$ , the integral can be evaluated, and we find

$$\langle (s + \rho)^{\alpha-1} \rangle \sim \tau_r^\nu s^{\alpha+\nu-1} \frac{\Gamma(1 - \alpha - \nu)}{\Gamma(1 - \alpha)}, \quad \text{for } s\tau_r \ll 1. \quad (88)$$

Including the remaining factor of  $s$  in the denominator, we see that  $\hat{K}_d(s) \sim s^{-\alpha-\nu}$ . Due to the additional factor of  $r$  in the numerator of  $\hat{K}_r(s)$ , this numerator does not diverge, but tends to  $\langle \rho^\alpha \rangle$ . Thus, the reaction kernel  $\hat{K}_r(s) \sim \langle \rho^\alpha \rangle \tau_r^{-\nu} s^{-(\alpha+\nu)}$  and  $\hat{K}_d(s) \sim \tau_r^{-\nu} s^{-(\alpha+\nu)}$ . These kernels provide the Laplace-space definitions of the fractional derivative of order  $1 - (\alpha + \nu)$  in (42).

### E. Random rate model for $\langle \tau \rangle < \infty$

We have seen that for  $\langle \tau \rangle < \infty$ , the system is perfectly well-mixed in the scaling limit. However, when  $\tau_m > 0$ , the degree of mixing varies. Details of the rate and waiting-time distributions appear in the survival probability  $p(t)$ , and the solutions are rather complicated.

The following example offers a good illustration of how the system goes from well-mixed to poorly-mixed as  $\tau_m$  increases. We assume exponentially distributed waiting times and  $n$  discrete decay rates  $\{r_i\}$ , and find that  $p(t)$  decays as a sum of  $n$  exponentials whose rates  $\{b_i\}$  cannot be easily computed in general.  $p(t)$  decays at long times as the slowest of these rates. We assume exponentially distributed waiting times with density

$$\psi_\tau(t) = (1/\tau_m) \exp(-t/\tau_m), \quad (89)$$

so that  $\langle \tau \rangle = \tau_m$ . Then  $p(t)$  in Laplace space becomes

$$\hat{p}(s) = \frac{\langle \frac{1 - \hat{\psi}_\tau(s+\rho)}{s+\rho} \rangle}{\langle 1 - \hat{\psi}_\tau(s+\rho) \rangle} = \tau_m \frac{\langle \frac{1}{1 + \tau_m(s+\rho)} \rangle}{1 - \langle \frac{1}{1 + \tau_m(s+\rho)} \rangle}. \quad (90)$$

Note that in (90), *no* approximations have been made. The density of discrete rates is given by

$$\rho(r) = \frac{1}{n} [\delta(r - r_1) + \delta(r - r_2) + \dots + \delta(r - r_n)], \quad (91)$$

where we have chosen equal weights for simplicity. Substituting (91) into (90), we find

$$p(s) = \frac{\frac{1}{1+(s+r_1)\tau_m} + \frac{1}{1+(s+r_2)\tau_m} + \dots}{\frac{s+r_1}{1+(s+r_1)\tau_m} + \frac{s+r_2}{1+(s+r_2)\tau_m} + \dots} \quad (92)$$

Putting all terms in the numerator over a common denominator and likewise with all terms in the denominator and then canceling the common denominator, we arrive at a fraction with a polynomial of order  $n - 1$  in  $s$  in the numerator and a polynomial of order  $n$  in  $s$  in the denominator. Note that if we rewrite the following expression with a common denominator

$$\frac{a_1}{s + b_1} + \frac{a_2}{s + b_2} + \dots + \frac{a_n}{s + b_n}. \quad (93)$$

we obtain again a fraction with a polynomial of order  $n - 1$  in the numerator and  $n$  in the denominator. Because inverting this last expression gives a sum of exponentials, inverting (92) also gives a sum of exponentials. (There can be no oscillating modes.) The decay rates of  $p(t)$  are found by equating coefficients in the two expressions (92) and (93), with the result that  $\{b_i\}$  are given by the roots of the polynomial in  $s$

$$\sum_{j=1}^n (s - r_j) \prod_{i \neq j} (1 + [s - r_i] \tau_m). \quad (94)$$

Dividing (94) by  $\tau_m^{n-1}$  and expanding about  $1/\tau_m = 0$ , we find that for  $\tau_m \gg 1/r_j$ ,  $j = 1, \dots$ , the effective rates are equal to the discrete disordered rates  $\{b_i\} = \{r_i\}$ . This is the poorly-mixed and highly-segregated limit. Each particle decays in its initial environment. At long times,  $p(t)$  decays exponentially at the rate equal to the smallest of  $\{r_i\}$ .

In the opposite limit  $\tau_m \ll 1/r_j$ ,  $j = 1, \dots$ , the polynomial (94) has singular roots. The roots may be found by regular perturbation after substituting  $y = s\tau_m$  and multiplying by  $\tau_m$ , so that (94) becomes, to leading order in  $\tau_m$

$$\left( \tau_m \sum_{j=1}^n r_j - ny \right) (1 - y)^{n-1}.$$

Thus, the roots are  $s = \langle \rho \rangle$ , and the  $(n - 1)$ -fold degenerate value  $s = 1/\tau_m$ . This shows how the well-mixed limit of a single homogeneous rate  $\langle \rho \rangle$  is approached with increasing  $\tau_m$ . All modes except the homogeneous mode decay rapidly. Only the homogeneous mode survives the scaling limit  $\tau_m \rightarrow \infty$ , so the decay is purely exponential for all times. For  $n = 2$  the rates of the multi-exponential decay of  $p(t)$  take the explicit form

$$\frac{1}{2\tau_m} \left[ 1 + \tau_m(r_1 + r_2) \pm \sqrt{\tau_m^2(r_1 - r_2)^2 + 1} \right], \quad (95)$$

which shows that transport and decay are coupled in the intermediate regime. The coefficients of the two terms corresponding to the rates (95) are

$$\frac{1}{2} \{ 1 \mp [1 + \tau_m^2(r_1 - r_2)^2] \}.$$

We see that, as  $\tau_m \rightarrow 0$  the coefficient corresponding to the rate that diverges as  $1/\tau_m$  tends to zero.

Finally, we note that the example above is the solution for the survival time of the first passage time under reset process, with the density of the underlying FPT given by (91), and exponentially distributed reset time.

### F. Stochastic simulations

We verify and illustrate the analytic results using stochastic simulations of the microscopic model as pre-



sented in Sec. II. The analytic results are plotted using exact asymptotic expansions as well as numerical inverse Laplace transform (ILT) of the solutions in Laplace space. The simulation curves represent averages over  $10^6 - 10^8$  trials. Inverse Laplace transform is used in Figs. 2, 3, 4, 5, and 6. Dashed and dotted lines in these figures are obtained from real-space asymptotic expansions. Stochastic simulations are used in Figs 3 and 5. These figures clearly show excellent agreement between theoretical predictions and simulations of the microscopic model.

The analytic results are mostly based on limiting forms of the PDFs for large or small arguments. For simulations, and ILT, we used the following concrete PDFs. To represent the heavy-tailed waiting time density (33), we choose the Pareto distribution.

$$\psi_\tau(t) = \begin{cases} \alpha\tau_m^\alpha/\Gamma(1-\alpha)t^{-\alpha-1} & \text{for } t > \tau_m\Gamma(1-\alpha)^{-1/\alpha} \\ 0 & \text{otherwise} \end{cases}. \quad (96)$$

To represent the rate PDF (40) for Fig. 2, we used the upper-truncated density

$$\psi_\rho(r) = \begin{cases} \nu r_0^{-\nu} r^{\nu-1} & r < r_0 \\ 0 & \text{otherwise} \end{cases}, \quad (97)$$

where  $r_0 = \tau_r^{-1}\Gamma(\nu+1)^{1/\nu}$ , and  $\psi_\rho^*(z) \equiv 1$ . For the other figures we instead used the gamma distribution, which is exactly (40) with  $\psi_\rho^*(z) = \exp(-z)$ . In accordance with the discussion leading to (2), we also sampled from the PDF for  $\Delta$  directly. For the gamma distribution, the integral  $\psi_\Delta(t) = \langle \rho \exp(-\rho t) \rangle$  takes the form

$$\psi_\Delta(t) = \nu\tau_r^{-1}(1+t/\tau_r)^{-\nu-1}. \quad (98)$$

It is well known that one can easily sample from a distribution if its cumulative distribution function (CDF) can be inverted. The CDF corresponding to (98) is  $C(t) = 1 - (1+t/\tau_r)^{-\nu}$ . The functional inverse is  $t(C) = \tau_r[(1-C)^{-1/\nu} - 1]$ . Samples of the PDF (98) are obtained by substituting pseudo-random numbers uniformly distributed on  $(0, 1)$  for  $C$  in  $t(C)$ .

The curves in Fig. 3 that were obtained by numerical inversion are based on (38). The corresponding Monte Carlo (MC) curves in the same figure were obtained by averaging  $10^6 - 10^7$  trials of the microscopic model. The rates were sampled from a gamma distribution with mean 1, and a microscopic timescale  $\tau_m = 1/100$ . Thus, systematic deviations of the MC from the scaling limit (38) are not visible in Fig. 3.

Fig. 5 verifies the expression for the MSD  $m(t)$  given by (70) with waiting time PDF characterized by  $\alpha = 1/4$ ,  $\tau_m = 0.1$ , and two equally probable rates, 0 and  $\tau_r$ , represented by the rate PDF (54) with  $p = 1/2$ . We show curves for two values of  $\tau_r$ ,  $\tau_r = 10^3$ , and  $\tau_r = 10^4$ . The curves compare ILT with averages over  $1.5 \times 10^7$  simulations. Due to statistical noise, it is difficult to probe the long time behavior of  $m(t)$  in the scaling

limit with simulations. Deviation from the scaling limit is clearly visible in Fig. 5. On this double-log plot, the curves would be linear for  $t < \tau_r$  in the scaling limit. In particular, they would coincide with the scaling limit of  $m(t)$  for the non-reactive CTRW shown in Fig. 2. To obtain agreement with the simulations on the scale of this plot, it is sufficient to include the first correction to the scaling limit of (70) for the ILT. As expected, the crossover to localized behavior clearly occurs for  $t \approx \tau_r$ .

### 1. Survival probability.

Here we present the method and algorithm used to compute an MC estimate of the survival probability  $p(t)$  from simulations. The survival probability can be written

$$p(t) = 1 - \int_0^t p_d(t') dt' = 1 - C_d(t), \quad (99)$$

where  $p_d(t)$  is the probability density for the death time, and  $C_d(t)$  is the cumulative distribution function (CDF) of the death time. To make clear the meaning of death time: the probability that a particle dies between time  $t$  and  $t + dt$  is  $p_d(t) dt$ , given that is alive and untrapped at time  $t = 0$ . We compute the empirical CDF corresponding to  $C_d(t)$ , which is an unbiased estimator that converges to  $C_d(t)$  [66].

The empirical CDF of the CDF  $C(x)$  of a random variable  $X$  is computed as follows. 1) Draw  $n$  independent samples of  $X$ , storing each one in an array  $A$  in sampling order. 2) Sort the array  $A$  in increasing order. In particular, after sorting, the first element  $A_1$  is the least sample and the last element  $A_n$  is the greatest sample. The empirical CDF is given by the points  $(A_i, i/n)$ . To be clear, the coordinate is  $A_i$  and the ordinate is  $i/n$ . Referring to (99), the empirical survival probability is given by  $(A_i, 1 - i/n)$ .

### 2. Mean square displacement.

We compute MC estimates as follows. The time increments of a particle's trajectory and its death time are generated as in the previous section. However, we also track the position of the walker at each step, using normally distributed step displacements with unit variance. In order to perform an ensemble average over trajectories, we must establish an array of fixed times  $t_{\text{rec}}$  at which to record the MSD. We also maintain an array  $m_{\text{rec}}$  of the same length. The element  $m_{\text{rec},i}$  contains the sum over particle trajectories of the squared displacement recorded at time  $t_{\text{rec},i}$ . We consider, as before, two cases. Either the walker dies during a step, or does not. Consider the second case. The walker is at position  $x = \sum_{j=1}^{i-1} x_j$  during the time interval  $(t, t + t_i)$ . We maintain an index  $i_m$  into the array  $t_{\text{rec}}$  corresponding the most recent time at which the squared displacement for this trajectory was

recorded. We then check which of the recording times  $t_{\text{rec},i_m+1}, t_{\text{rec},i_m+2}, \dots$  lie in the interval  $(t, t + t_i)$ . For each of the corresponding indices  $i_m + 1$ , etc. we add  $x^2$  to the element  $m_{\text{rec},i_m+1}$ , etc. We advance  $i_m$  to the last recorded time. We then proceed to the next step. Now consider the first case, when the particle dies. The relevant time interval is now  $(t, t + \delta t)$ , because the particle dies at  $t + \delta t$ . We only record  $x^2$  at recording times lying in this final interval. In both cases, we also increment the number of particle trajectories  $n_i$  contributing to the sum at each recording time  $t_{\text{rec},i}$ . This number of course decreases with increasing time because particles are dying. The estimate of the MSD normalized by the survival probability is then  $m_{\text{rec},i}/n_i$ . Suppose the total number of trials is  $n$ . The estimate of the MSD normalized by the total number of particles, live or dead is of course

$m_{\text{rec},i}/n$ . The relation to the analytic quantities is

$$\int_{-\infty}^{\infty} dx x^2 p(x, t) \Leftrightarrow m_{\text{rec},i}/n, \quad (100)$$

and

$$m(t) = \frac{\int_{-\infty}^{\infty} dx x^2 p(x, t)}{\int_{-\infty}^{\infty} dx p(x, t)} \Leftrightarrow m_{\text{rec},i}/n_i. \quad (101)$$

As an example to understand the difference: Suppose only live particles are detectable. Then  $m(t)$  describes the observed width of the cloud. Note that the corresponding estimate of  $p(t)$  is  $n_i/n$ , so that we have, as expected  $(m_{\text{rec},i}/n)/(n_i/n) = m_{\text{rec},i}/n_i$ . In practice, we instead estimate  $p(t)$  using the method described in the previous section, which is far more efficient. We used the Mersenne Twister RNG.

## ACKNOWLEDGMENTS

This work was supported by the European Research Council (ERC) through the project MHetScale (Contract number 617511)

- 
- [1] M. von Smoluchowski, *Z. Phys. Chem.* **92**, 129 (1917).  
 [2] A. Ovchinnikov and Y. Zeldovich, *Chem. Phys.* **28**, 215 (1978).  
 [3] O. Bénichou, D. Grebenkov, P. Levitz, C. Loverdo, and R. Voituriez, *Phys. Rev. Lett.* **105**, 150606 (2010).  
 [4] S. Reuveni, R. Granek, and J. Klafter, *Phys. Rev. E* **82**, 041132 (2010).  
 [5] S. Reuveni, R. Granek, and J. Klafter, *Phys. Rev. E* **81**, 040103 (2010).  
 [6] D. ben Avraham and S. Havlin, *Diffusion and Reactions in Fractals and Disordered Systems* (Cambridge University Press, Cambridge, 2005).  
 [7] C. I. Steefel, D. J. DePaolo, and P. C. Lichtner, *Earth and Planetary Science Letters* **240**, 539 (2005).  
 [8] M. Dentz, T. LeBorgne, A. Englert, and B. Bijeljic, *J. Cont. Hydrol.* **120-121**, 1 (2011).  
 [9] S. Schnell and T. Turner, *Prog. Biophys. Mol. Bio.* **85**, 235 (2004), modelling Cellular and Tissue Function.  
 [10] R. Kopelman, *J. Stat. Phys.* **42**, 185 (1986).  
 [11] M. A. Savageau, *J. Theor. Bio.* **176**, 115 (1995).  
 [12] D. Bratsun, D. Volfson, L. S. Tsimring, and J. Hasty, *PNAS* **102**, 14593 (2005).  
 [13] T. Brett and T. Galla, *Phys. Rev. Lett.* **110**, 250601 (2013), arXiv:1302.7166 [cond-mat.stat-mech].  
 [14] T. Tian, *PLoS One* **9** (2013), 10.1371/journal.pone.0052029.  
 [15] R. Aris and G. Astarita, *Chem. Eng. Process.* **26**, 63 (1989).  
 [16] S. Fedotov and V. m. c. Méndez, *Phys. Rev. E* **66**, 030102 (2002).  
 [17] Méndez, V., Ortega-Cejas, V., and Casas-Vázquez, J., *Eur. Phys. J. B* **53**, 503 (2006).  
 [18] B. I. Henry and S. L. Wearne, *Physica A* **276**, 448 (2000).  
 [19] B. I. Henry and S. L. Wearne, *SIAM Journal on Applied Mathematics* **62**, 870 (2002).  
 [20] B. I. Henry, T. A. M. Langlands, and S. L. Wearne, *Phys. Rev. E* **72**, 026101 (2005).  
 [21] T. A. M. Langlands, B. I. Henry, and S. L. Wearne, *Journal of Physics: Condensed Matter* **19**, 065115 (2007).  
 [22] I. M. Sokolov, M. G. W. Schmidt, and F. Sagués, *Phys. Rev. E* **73**, 031102 (2006), cond-mat/0510354.  
 [23] C. Meile and K. Tuncay, *Adv. Water Resour.* **29**, 62 (2006).  
 [24] L. Li, C. I. Steefel, and L. Yang, *Geochim. Cosmochim. Acta* **72**, 360 (2008).  
 [25] A. Iomin and V. Méndez, *Phys. Rev. E* **88**, 012706 (2013).  
 [26] C. Manzo, J. a. Torreno-Pina, P. Massignan, G. J. Lapeyre, M. Lewenstein, and M. F. Garcia Parajo, *Phys. Rev. X* **5**, 011021 (2015).  
 [27] D. D. Boehr, R. Nussinov, and P. E. Wright, *Nat. chem. biol.* **5**, 789 (2009).  
 [28] G. J. Lapeyre and M. Dentz, “quenched disorder walk,” In preparation.  
 [29] A. Pal and S. Reuveni, *Phys. Rev. Lett.* **118**, 030603 (2017), arXiv:1607.06048 [cond-mat.stat-mech].  
 [30] D. T. Gillespie, *J. Phys. Chem.* **81**, 2340 (1977).  
 [31] N. van Kampen, *Stochastic Processes in Physics and Chemistry*, 3rd ed. (Elsevier, Amsterdam, 2007).  
 [32] S. Reuveni, *Phys. Rev. Lett.* **116**, 170601 (2016), arXiv:1512.01600 [cond-mat.stat-mech].  
 [33] J. Klafter and I. M. Sokolov, *First Steps in Random Walks* (Oxford University Press, Oxford, 2011).  
 [34] I. M. Sokolov, *Soft Matter* **8**, 9043 (2012).

- [35] J.-P. Bouchaud and A. Georges, *Phys. Rep.* **195**, 127 (1990).
- [36] R. Metzler, J.-H. Jeon, A. G. Cherstvy, and E. Barkai, *Phys. Chem. Chem. Phys.* **16**, 24128 (2014).
- [37] F. Sabzikar, M. M. Meerschaert, and J. Chen, *J. Chem. Phys.* **293**, 14 (2015).
- [38] R. Metzler and J. Klafter, *J. Math. Phys. A* **37**, R161 (2004).
- [39] F. Sagués, V. P. Shkilev, and I. M. Sokolov, *Phys. Rev. E* **77**, 032102 (2008), arXiv:0712.1436.
- [40] E. Abad, S. B. Yuste, and K. Lindenberg, *Phys. Rev. E* **81**, 031115 (2010), arXiv:0911.3137 [cond-mat.stat-mech].
- [41] S. Fedotov, *Phys. Rev. E* **81**, 011117 (2010).
- [42] Abad, E., Yuste, S. B., and Lindenberg, K., *Math. Model. Nat. Phenom.* **8**, 100 (2013).
- [43] S. B. Yuste, E. Abad, and K. Lindenberg, *Phys. Rev. Lett.* **110**, 220603 (2013), arXiv:1304.7534 [cond-mat.stat-mech].
- [44] B. I. Henry, T. A. M. Langlands, and S. L. Wearne, *Phys. Rev. E* **74**, 031116 (2006).
- [45] E. Abad, S. B. Yuste, and K. Lindenberg, *Phys. Rev. E* **88**, 062110 (2013), arXiv:1309.7699 [cond-mat.stat-mech].
- [46] L. R. Kump, S. L. Brantley, and M. A. Arthur, *Annual Review of Earth and Planetary Sciences* **28**, 611 (2000).
- [47] C. Peters, J. Lewandowski, M. Maier, M. Celia, and L. Li, in *XVI International Conference on Computational Methods in Water Resources* (2006).
- [48] S. K. Hansen and B. Berkowitz, *Phys. Rev. E* **91**, 032113 (2015).
- [49] M. M. Meerschaert and P. Straka, *Ann. Probab.* **42**, 1699 (2014).
- [50] T. Appuhamillage and V. Bokil, *Ann. Appl. Probab.* **21**, 183 (2011).
- [51] J. Ramirez, E. Thomann, and E. Waymire, *Statistical Science* **28**, 487 (2013).
- [52] S. C. Kou, B. J. Cherayil, W. Min, B. P. English, and X. S. Xie, *J. Phys. Chem. B* **109**, 19068 (2005).
- [53] M. A. Lomholt, M. Urbakh, R. Metzler, and J. Klafter, *Phys. Rev. Lett.* **98**, 168302 (2007), q-bio/0611011.
- [54] R. Grima, *Phys. Rev. Lett.* **102**, 218103 (2009).
- [55] O. Pulkkinen and R. Metzler, *Sci. Rep.* **5**, 17820 (2015).
- [56] A. B. Kolomeisky, *J. Chem. Phys.* **134**, 155101 (2011), arXiv:1101.4330 [cond-mat.stat-mech].
- [57] M. B. J. Roeffaers, B. F. Sels, H. Uji-i, F. C. De Schryver, P. A. Jacobs, D. E. De Vos, and J. Hofkens, *Nature* **439**, 572 (2006).
- [58] J. Wu and J. Cao, “Generalized Michaelis–Menten equation for conformation-modulated monomeric enzymes,” in *Single-Molecule Biophysics*, edited by T. Komatsuzaki, M. Kawakami, S. Takahashi, H. Yang, and R. J. Silbey (John Wiley & Sons, Inc., Hoboken, 2011) pp. 329–365.
- [59] S. Reuveni, M. Urbakh, and J. Klafter, *PNAS* **111**, 4391 (2014).
- [60] T. Rotbart, S. Reuveni, and M. Urbakh, *Phys. Rev. E* **92**, 060101 (2015), arXiv:1509.05071 [cond-mat.stat-mech].
- [61] K. P. F. Janssen, G. De Cremer, R. K. Neely, A. V. Kubarev, J. Van Loon, J. A. Martens, D. E. De Vos, M. B. J. Roeffaers, and J. Hofkens, *Chem. Soc. Rev.* **43**, 990 (2014).
- [62] E. Barkai, Y. Garini, and R. Metzler, *Phys. Today* **65**, 29 (2012).
- [63] M. J. Morelli, R. Allen, and P. R. ten Wolde, *Biophys. J.* **101**, 2882 (2017).
- [64] G. Guigas and M. Weiss, *Biophys. J.* **94**, 90 (2008).
- [65] H.-X. Zhou, G. Rivas, and A. P. Minton, *Ann. Rev. Biophys.* **37**, 375 (2008).
- [66] P. Billingsley, *Probability and Measure*, 3rd ed. (John Wiley and Sons, New York, 1995).